Simulation Modelling Practice and Theory 133 (2024) 102912

Contents lists available at ScienceDirect

Simulation Modelling Practice and Theory

journal homepage: www.elsevier.com/locate/simpat

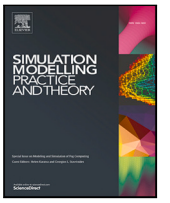

Efficient derivation of optimal signal schedules for multimodal intersections

Nicola Bertocci, Laura Carnevali *, Leonardo Scommegna, Enrico Vicario

Department of Information Engineering, University of Florence, via di Santa Marta 3, Florence, Italy

A R T I C L E I N F O

Dataset link: https://doi.org/10.5281/zenodo.10693840, https://doi.org/10.5281/zenodo.10695718

Keywords:
Multimodal intersections
Optimal signal schedules
Stochastic Time Petri nets (STPNs)
Finite-capacity vacation queues with general vacation time
Simulation of Urban MObility (SUMO)

A B S T R A C T

Tramways decrease time, cost, and environmental impact of urban transport, while requiring multimodal intersections where trams arriving with nominal periodic timetables may have right of way over road vehicles. Quantitative evaluation of stochastic models enables early exploration and online adaptation of design choices, identifying operational parameters that mitigate impact on road transport performance.

We present an efficient analytical approach for offline scheduling of traffic signals at multimodal intersections among road traffic flows and tram lines with right of way, minimizing the maximum expected percentage of queued vehicles of each flow with respect to sequence and duration of phases. To this end, we compute the expected queue size over time of each vehicle flow through a compositional approach, decoupling analyses of tram and road traffic. On the one hand, we define microscopic models of tram traffic, capturing periodic tram departures, bounded delays, and travel times with general (i.e., non-Exponential) distribution with bounded support, open to represent arrival and travel processes estimated from operational data. On the other hand, we define macroscopic models of road transport flows as finite-capacity vacation queues, with general vacation times determined by the transient probability that the intersection is available for vehicles, efficiently evaluating the exact expected queue size over time. We show that the distribution of the expected queue size of each flow at multiples of the hyperperiod, resulting from temporization of nominal tram arrivals and vehicle traffic signals, reaches a steady state within few hyper-periods. Therefore, transient analysis starting from this steady-state distribution and lasting for the hyper-period duration turns out to be sufficient to characterize road transport behavior over time intervals of arbitrary duration.

We implemented the proposed approach in the novel OMNIBUS Java library, and we compared against Simulation of Urban MObility (SUMO). Experimental results on case studies of real complexity with time-varying parameters show the approach effectiveness at identifying optimal traffic signal schedules, notably exploring in few minutes hundreds of schedules requiring tens of hours in SUMO.

1. Introduction

1.1. Motivation

The growing need of urban mobility promotes development of tramways [1] to reduce traffic congestion and improve quality of service and environmental sustainability of transport [2,3]. However, tramways also reduce resources for road traffic and in

* Correspondence to: via di Santa Marta 3, 50139 Firenze, Italy
E-mail addresses: nicola.bertocci@unifi.it (N. Bertocci), laura.carnevali@unifi.it (L. Carnevali), leonardo.scommegna@unifi.it (L. Scommegna), enrico.vicario@unifi.it (E. Vicario).

https://doi.org/10.1016/j.simpat.2024.102912
Received 20 November 2023; Received in revised form 12 February 2024; Accepted 18 February 2024
Available online 20 February 2024

particular require multimodal intersections where trams typically have right of way. Optimization of traffic signals becomes crucial to mitigate the impact. To this end, quantitative evaluation of stochastic models combining arrival and service processes of road traffic and tramway flows can effectively support early assessment of design choices and runtime adaptation, leveraging smart technologies for online estimation of traffic parameters and tram delays with respect to nominal arrival times [4] to maximize expected capacity or minimize expected queue lengths and delays due to signal control at intersections [5].

1.2. Related works

Various methods for operation and management of urban transportation systems address simulation and analysis of traffic signals [6], leveraging models such as variants of Petri Nets (PNs) [7], cellular automata [8], and car following representations [9]. These models are defined at different levels of abstraction, ranging from microscopic to macroscopic: on the one hand, *microscopic models* represent behavior of individual vehicles, possibly capturing interactions among vehicles and fine details about driver actions (e.g., reaction and impatience); on the other hand, *macroscopic models* encode global or aggregated features of traffic streams (e.g., density, flow, and average speed), typically achieving computational efficiency while structurally missing the representation of synchronous phenomena like tram arrivals. These models are evaluated by various simulative and analytical solution techniques such as the input–output method [10], the shockwave theory [11,12], and rule-based methods [13,14], typically computing various mobility and sustainability measures, such as expected queue lengths and waiting times at intersections, and expected fuel consumption [6].

In the literature on macroscopic models, an urban intersection is modeled in [15] as a Hybrid Petri Net (HPN), where the continuous dynamics represents road traffic flows and the discrete dynamics models traffic light rules, comparing vehicles flows computed through HPN simulation with real traffic data. The model is extended in [16] to represent an urban transportation network made of multiple intersections, solving a control problem to coordinate the traffic lights of several intersections so as to minimize the travel time of a special class of road vehicles. An urban intersection among road traffic flows is modeled in [17] through a variant of HPNs, representing vehicle flows as fluids and lane interruptions and traffic light signals as discrete events, and computing the average number of vehicles in each link via model simulation. In [18], Petri nets are used to synthesize both microscopic and macroscopic models of multiple signalized intersections among road traffic flows, assuming Poisson arrivals, and exploiting adaptive spatial discretization and model simulation to derive flow rate and speed of vehicles. A macroscopic model of a traffic network consisting of signalized and unsignalized intersections is defined in [19] by capturing the vehicle flow dynamics at each intersection, solving a mixed integer linear programming problem to derive an optimal traffic light control strategy. The input–output approach [20] estimates vehicle arrival and departure profiles at signalized intersections among vehicle flows to predict delay (i.e., difference between actual and desired travel time) and maximum queue length over time for each vehicle flow for each signal cycle, assuming that temporization of traffic signals is a-priori known, and that the queue rear does not exceed vehicle detector, preventing application to congestion scenarios. In [12], the shockwave theory is used to analyze the dynamics of formation and dissipation of queues at isolated signalized intersections among vehicle flows by examining the dynamics of the shock waves formed due to intermitted service of traffic, achieving accuracy in temporal and spatial characterization of queueing processes and in identification of the optimal cycle, while assuming that vehicle arrival times are known and have binomial distribution. Results are extended in [21] using existing detectors to estimate the maximum queue length (i.e., distance from the intersection stop line to the position of the last vehicle that has to stop in a cycle), managing congested links with long queues while requiring high resolution of traffic signal data.

In the literature on microscopic models, detection and solution of conflicts induced by driver behavior at multiple signalized intersections is supported in [22] by models in the class of Time Petri Nets (TPNs), representing deterministic durations of traffic light phases, periodic arrival times of vehicles, and uncertain travel times comprised within min–max intervals, but without associating temporal parameters with a measure of probability. The model is extended in [23] into a Deterministic and Stochastic Petri Net (DSPN) where normal distributions of vehicle flows and travel times are approximated with Erlang distributions, supporting deadlock detection through structural DSPN analysis and minimization of queue lengths through the optimal setting of the durations of traffic light phases within a receding horizon approach. In particular, DSPN simulation is exploited to derive mean queue lengths during 5-minute intervals, assuming that the sequence of phases is fixed and a-priori known. Preliminary results on the analysis of a microscopic model of an intersection between a vehicle flow and a two-track tram line with right of way are presented in [24,25]. The model features periodic tram departures and stochastic tram delays and travel times, but explicitly represents each state of the queue of vehicles, so that the evaluation does not scale with the queue size and is limited to deriving a rough estimate on the average queue size over time by grouping car arrivals into platoons. In [13], rule-based simulation of different signal policies at a signalized intersection is performed under different traffic demands to evaluate how transit vehicles with right of way impact other traffic flows, assuming Poisson vehicle arrivals, considering traffic light schedules with fixed phase sequence, and not representing synchronous arrivals and distributions of travel times. Model predictive control policies are developed in [26] for two connected multi-modal signalized intersections between vehicles and bicycles, exploiting simulation of an analytical model representing average time-dependent arrival rates, number of queued vehicles, number of queued bicycles, and traffic signals with fixed phase sequence, while not associating arrival and travel processes with a stochastic characterization. A deterministic model of two connected signalized intersections is defined also in [27], solving a mixed integer linear programming problem to accommodate asynchronous priority requests from different modes of vehicles and pedestrians, and implementing the proposed traffic control policy using the VISSIM microscopic simulation tool [28,29]. Mixed linear integer programming problems exploiting similar deterministic models are solved also to coordinate tram timetables and signal timing at intersections with vehicle flows, aiming at minimizing tram travel times and

maximizing tram timetable adherence, either exploiting emerging technologies such as automatic vehicle location and advanced control systems [30] or predetermining signal coordination based on volumes and operational characteristics of transit vehicles [31]. Similarly, a multi-objective optimization problem is solved also in [32] to minimize tram travel times and dwell times for a single two-way line, aiming also at minimizing impact of trams on road vehicles at signalized intersections, though considering a simple model where same transit signal priority actions have same negative effect (cost) regardless of traffic conditions. Simulation of an urban mobility model based on cellular automata is used in [33] to investigate how traffic is affected by control mechanisms at signalized intersections, such as cycle duration, green split, and coordination of traffic signals, assuming a single mode of transport and considering a simplified scenario where the network topology consists of evenly spaced horizontal and vertical streets, and each direction has the same traffic load and thus also the same amount of green time at any intersection. Simulation of stochastic cellular automata is used in [34] to compare tram priority schemes at signalized intersections with road vehicle traffic, considering vehicle turning probability and tram stopping probability, while assuming tram arrivals at deterministic times not subject to stochastic delays.

Other methods exploit autonomy and connectivity in vehicle technology as well as road sensors detecting vehicle movements to optimize traffic signal control at signalized intersections [35], thus addressing significantly different scenarios with respect to our approach which just assumes the presence of sensors to detect tram passages, e.g., joint optimization of signal control and vehicle paths is performed to minimize vehicle delay under homogeneous traffic of fully automated vehicles in [36] and under mixed traffic of automated and conventional vehicles in [37]; real-time synchronous management of vehicle movements is performed in [38] to reduce travel delay and fuel consumption; and, in [39], an offline planner, resynchronizing traffic signals to minimize tram travel times, is integrated with an online controller, adopting different control strategies to instruct trams to travel within appropriate progressions. Various approaches at different scale of abstraction exploit machine learning methods for traffic signal control [6,40], such as multi-agent learning and reinforcement learning [41–43], requiring availability of significantly larger amounts of mobility data with respect to our approach, for which statistics of inter-arrival and travel times of vehicles and trams are sufficient for model definition. According to this, these classes of related works are regarded as out of scope with respect to this paper.

1.3. Contribution

In this paper, we present an efficient and accurate analytical approach for offline scheduling of traffic signals at multimodal intersections among road transport flows and tram lines with right of way, aimed at minimizing the maximum expected percentage of queued vehicles of each flow with respect to sequence and duration of phases. To this end, we derive the expected queue size over time of each vehicle flow through a compositional approach which decouples analyses of a microscopic model of tram traffic and a macroscopic model of road traffic, notably achieving accuracy comparable with that of SUMO (Simulation of Urban MObility) [44] in finding optimal schedules while significantly outperforming it in terms of computational load. To the best of our knowledge, this is the first paper where optimization of traffic signals at vehicle-tram intersections is addressed by capturing periodic tram departures and general (GEN), i.e., non-Exponential, tram delays and travel times, with consequent unavailability of the intersection to vehicle flows for time intervals having GEN duration, starting from periodic time instants subject to GEN delays. Specifically:

- We provide a microscopic model of tram traffic using Stochastic Time Petri Nets (STPNs) [45], representing periodic inter-arrival times as well as GEN bounded delays and crossing times, opening the way to the representation of arrival and travel processes estimated from operational data, and thus also to the integration of model-based and data-driven approaches. We perform numerical analysis based on the method of stochastic state classes [46] to compute the transient probability that the intersection is available for vehicle flows.
- We provide a macroscopic model of vehicle traffic by finite-capacity vacation queues [47–49], with GEN vacation times (i.e., duration of the intervals of intersection unavailability for vehicles) determined by the transient probability that the intersection is unavailable for vehicle flows, and with Exponential (EXP) inter-arrival times and service times (i.e., times needed to leave the intersection). Note that non-EXP inter-arrival times and service times could be easily modeled as well, e.g., using hyper-EXP distributions, Markovian Arrival Processes, and time-inhomogeneous Poisson Processes, enabling representation of vehicles arriving in bursts, platoons, and free flow. We solve the set of ordinary differential equations characterizing the queue behavior to derive the expected queue size over time for each flow. Note that derivation is exact, given that dependencies of vehicle traffic on tram traffic are taken into account in the evaluation.
- We prove that the distribution of the expected queue size of each vehicle flow reaches a steady state at multiples of the hyper-period, resulting from temporization of nominal tram arrivals and vehicle traffic signals. We derive this distribution by performing steady-state analysis of the Discrete Time Markov Chain (DTMC) embedded at multiples of the hyper-period in the continuous-time birth–death process characterizing the queue behavior. Given that the steady state is experimentally observed to be reached within few hyper-periods, the expected queue size over time can be derived by performing transient analysis starting from the steady-state distribution and lasting for the hyper-period duration.
- We compare with SUMO to assess accuracy and computational load of deriving signal schedules that minimize the maximum expected percentage of queued vehicles of each flow, considering road-tramway intersections of real complexity. Results show that the approach achieves comparable accuracy, while requiring a computation time up to nearly four orders of magnitude lower than that of SUMO, notably evaluating in few minutes hundreds of schedules requiring tens of hours in SUMO.

Summarizing, major contributions of this paper consist of: definition of an efficient and accurate approach for offline derivation of optimal signal schedules for multimodal intersections among road transport flows and tram lines with right of way, capturing periodic tram departures and GEN tram delays and travel times; comparison of experimental results with those obtained by SUMO; definition and implementation of a metamodel of a multimodal intersection, enabling automated model derivation and analysis; implementation of the approach in the OMNIBUS Java library available open source under the AGPLv3 licence at https://doi.org/10.5281/zenodo.10693840, supporting replication of the experimental results; and, implementation of a repository supporting replication of the comparison of the experimental results with those obtained by SUMO, available under the EPLv2 licence at https://doi.org/10.5281/zenodo.10695718.

1.4. Paper organization

The rest of the paper is organized in four sections. First, we define the metamodel of a multimodal urban intersection and we provide the STPN model of a metamodel instance (Section 2). Then, we perform transient analysis of the STPN model of each tram track to derive the transient probability that the intersection is available for vehicle flows, and we use this probability in the analysis of both transient and steady-state behavior of each vehicle flow to derive the expected queue size over time (Section 3). Next, we present experimental results (Section 4). Finally, we draw our conclusions (Section 5).

2. System model

In this section, we define the metamodel of a multimodal urban intersection (Section 2.1) and we represent metamodel instances through STPNs to provide them with formal semantics (Section 2.2).

2.1. Metamodel of a multimodal urban intersection

Fig. 1 shows the metamodel [50] of a multimodal urban intersection, capturing both the parameters of the STPN model of Section 2.2 and the parameters of the SUMO model used in Section 4 to validate experimental results. Table 1 summarizes all parameters, and Fig. 2 shows a schematic representation of an intersection (not representative of the geometry of the intersection). Specifically, we consider an intersection (represented by the class `Intersection`) among independent single-lane vehicle flows (class `VehicleFlow`) and independent tram lines with right of way (class `TramLine`), i.e., we consider unconditional transit signal priority control [51], according to which signal priority is granted based on the actual presence of trams. In the STPN model of Section 2.2 and in the SUMO model of Section 4, intersection crossing is regulated by a traffic light with periodic schedule σ with period P, also termed cycle [6], divided into W phases $\Sigma_1, \ldots, \Sigma_W$ with duration $B_1, \ldots, B_W$, respectively, such that during each phase either a subset of vehicle flows is allowed to cross the intersection unless a tram is approaching or crossing, or no vehicle flow is allowed to cross (e.g., for safety reasons when switching permission to cross among vehicle flows), i.e., $\sigma : [0, P] \to 2^{\{0,1,\ldots,I\}}$ where I is the number of vehicle flows and $i \in \sigma(t)$ if t belongs to a phase assigned to vehicle flow ϕ_i^{veh} and $\sigma(t) = \emptyset$ if t belongs to a phase during which no vehicle is allowed to cross the intersection. Similarly, we define the schedule σ_i of vehicle flow ϕ_i^{veh} as $\sigma_i : [0, P] \to \{0, 1\}$ where $\sigma_i(t) = 1$ if $i \in \sigma(t)$ and $\sigma_i(t) = 0$ otherwise. Moreover, in the SUMO model, an intersection has also length E, characterizing the distance that vehicles and trams must travel to cross it. For simplicity of presentation, we consider a single common length for each vehicle flow and tram line, though different lengths could be easily encompassed in the SUMO model.

Vehicles of each flow ϕ_i^{veh} queue up in a road section ahead of the traffic light (class `RoadSection`). In the SUMO model, the road section has length S_i and it allows vehicles of length C_i keeping safe distance D_i and maximum speed V_i. Therefore, the queue of ϕ_i^{veh} (class `Queue`) has capacity $K_i := \lfloor S_i/(C_i + D_i) \rfloor$, which is also a parameter of the STPN model. Both in the STPN model and in the SUMO model, for each vehicle flow ϕ_i^{veh}, the initial number of queued vehicles follows an arbitrary discrete probability distribution $\rho_i : \{0, 1, \ldots, K_i\} \to [0, 1]$, and vehicle arrivals are represented by a Poisson process with rate λ_i. When vehicles are allowed to cross the intersection by the traffic light schedule and no tram is approaching or crossing the intersection, the time needed by a vehicle of flow ϕ_i^{veh} to leave the intersection is characterized by an EXP distribution with rate $\mu_{i,k}$ in the STPN model. Note that non-EXP distributions of vehicle arrival times could be easily introduced both in the proposed approach and in SUMO (see Section 3.2), e.g., using hyper-EXP distributions, Markovian Arrival Processes, and time-inhomogeneous Poisson Processes, representing vehicles arriving in bursts, platoons, and free flow. Similarly, non-EXP distributions could be easily considered for vehicle leaving times in the proposed approach. As pointed out in Table 1, we remark that EXP leaving times are not enforced in SUMO in any way. Actually, in SUMO we just control the maximum vehicle speed V_i and the minimum vehicle distance D_i, e.g., vehicles may accelerate or decelerate when approaching or leaving the intersection.

Each tram line ϕ_l^{tram} consists of multiple tracks (class `TramTrack`). A wayside system is installed on each track, close to the intersection, to detect tram passages and trigger the traffic signals of vehicles red as the tram is approaching (the nominal periodic schedule σ of the intersection traffic light is restored when the tram has left the intersection). Both the STPN model and the SUMO model capture that trams of track $\phi_{l,z}^{\text{tram}}$ of line ϕ_l^{tram} reach the wayside system with nominal periodic inter-arrival times, with period T_l (same for all the tracks of the line) and offset $O_{l,z}$ (i.e., the nominal arrival time of the first tram is $O_{l,z}$ and that of the nth tram is $O_{l,z} + (n-1)\,T_l \;\forall\, n > 1$), and with delay having GEN distribution $d_{l,z} : [d_{l,z}^{\min}, d_{l,z}^{\max}] \to [0, 1]$ with bounded support. When traveling the short distance from the wayside system to the intersection, the tram speed is considered constant and thus the corresponding travel time is modeled as a deterministic (DET) value $G_{l,z}$, representing the time advance with which traffic signals of vehicles are

Table 1
Parameters of the STPN model and the SUMO model.

intersection parameter		STPN	SUMO
P	traffic signal period	✔	✔
B_w	duration of traffic signal phase Σ_w	✔	✔
E	intersection length	✗	✔
vehicle flow ϕ_i^{veh} parameter		**STPN**	**SUMO**
S_i	road section length	✗	✔
C_i	vehicle length	✗	✔
D_i	minimum vehicle distance	✗	✔
V_i	maximum vehicle speed	✗	✔
K_i	vehicle queue capacity	✔	✔
ρ_i	initial queue length distribution	✔	✔
λ_i	vehicle arrival rate	✔	✔
μ_i	vehicle leaving rate	✔	✗
tram line ϕ_l^{tram} parameter		**STPN**	**SUMO**
T_l	period	✔	✔
tram track $\phi_{l,z}^{\text{tram}}$ parameter		**STPN**	**SUMO**
$O_{l,z}$	offset	✔	✔
$d_{l,z}$	delay distribution	✔	✔
$G_{l,z}$	red signal trigger time	✔	✔
$c_{l,z}$	crossing time distribution	✔	✔

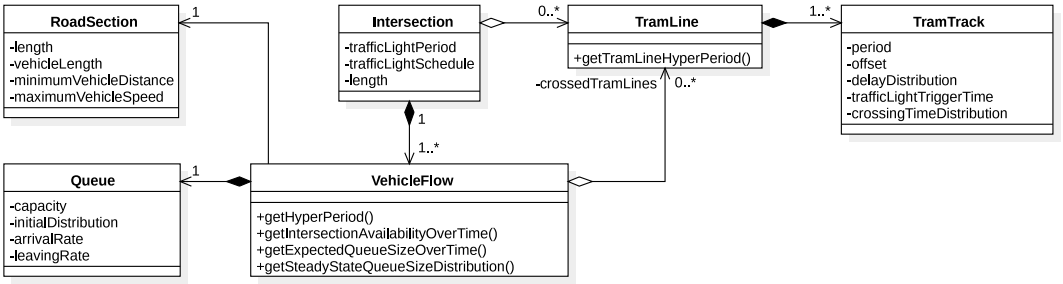

Fig. 1. Metamodel of intersections among independent vehicle flows and independent tram lines with right of way.

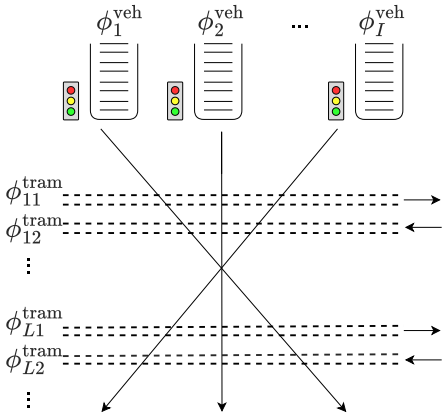

Fig. 2. Schematic representation of an intersection defined by the metamodel of Fig. 1.

triggered red with respect to the tram arrival time at the intersection. Conversely, the time needed by a tram to cross the intersection is characterized by a GEN distribution $c_{l,z} : [c_{l,z}^{\min}, c_{l,z}^{\max}] \to [0,1]$ with bounded support. Of course, the tram line period T_l is selected so that it is never the case that a tram approaches the intersection before the previous tram has left it, i.e., $T_l < O_{l,z} + d_{l,z}^{\max} + G_{l,z} + c_{l,z}^{\max}$ $\forall\, l \in \{1, \ldots, L\}$, $\forall\, z \in \{1, \ldots, Z_l\}$, where L is the number of tram lines and Z_l is the number of tracks of line ϕ_l^{tram}.

The *hyper-period* H of the intersection is the least common multiple of period P of traffic signals and periods $T_1, \ldots, T_L$ of tram lines $\phi_1^{\text{tram}}, \ldots, \phi_L^{\text{tram}}$, respectively.

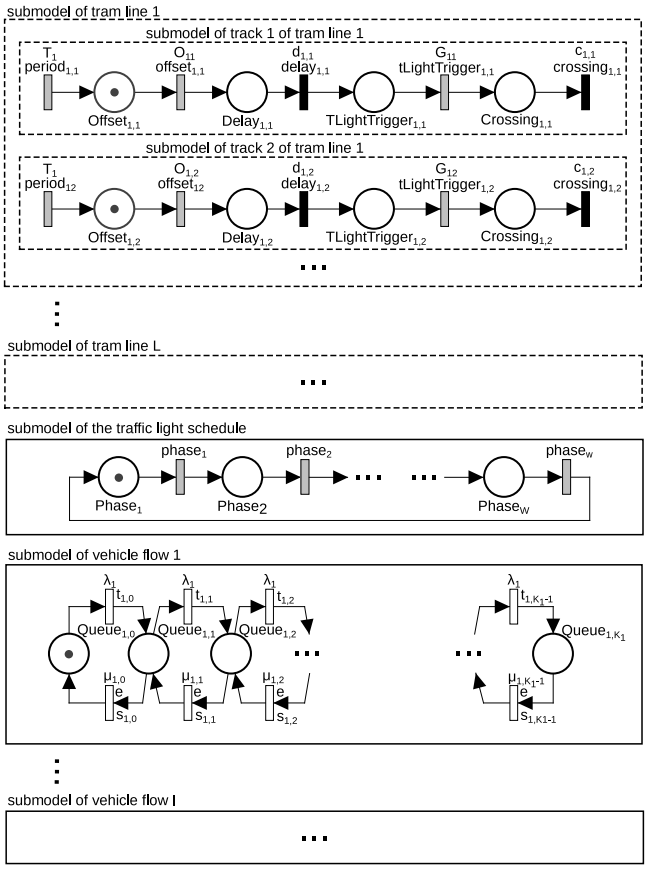

Fig. 3. STPN model of an instance of the metamodel of Fig. 1.

2.2. STPN of a multimodal urban intersection

Fig. 3 shows the STPN model of a multimodal urban intersection derived from the metamodel of Fig. 1. STPNs [45] model concurrent timed systems with stochastic temporal parameters and discrete probabilistic choices. Specifically, transitions (in Fig. 3, depicted as bars) model the stochastic duration of activities, tokens (depicted as dots) within places (depicted as circles) model the discrete logical state of the system, and directed arcs (depicted as directed arrows) from input places to transitions and from transitions to output places model precedence relations among activities. A transition is enabled by a marking (i.e., an assignment of tokens to places) if each of its input places contains at least one token and if its enabling function (depicted by label "e" and not shown to reduce the cluttering) evaluates to true (e.g., transition $\texttt{period}_{1,1}$ has neither input places nor enabling functions, and thus it is always enabled and it repeatedly fires at multiples of T_1, representing periodic tram arrivals of track $\phi_{1,1}^{\text{tram}}$). Upon enabling, each transition samples a time-to-fire from its Cumulative Distribution Function (CDF), which can be an EXP distribution (EXP transitions are depicted as tick white bars), a GEN distribution (GEN transitions are depicted as tick black bars), or the generalized distribution of a Dirac Delta function[1], in the latter case yielding DET time-to-fire (DET transitions are depicted as tick gray bars) or zero time-to-fire (transitions with zero time-to-fire, not present in Fig. 3, are depicted as thin black bars). The transition with minimum time-to-fire is selected to fire, removing one token from each of its input places and adding one token to each of its output places. Ties (i.e., limit cases of synchronization among DET transitions with same time-to-fire, e.g., occurring when transitions with the same DET value are enabled at the initial time) are solved by a random switch determined by probabilistic weights associated with transitions.

The model of Fig. 3 consists of a submodel for each track of each tram line, a submodel for the periodic schedule of the intersection traffic light, and a submodel for each vehicle flow. Specifically, the submodel of tram track $\phi_{l,z}^{\text{tram}}$ of line ϕ_l^{tram} consists of a sequence of transitions chained through their input places:

[1] To simplify presentation, without loss of generality, we do not provide a formal definition of generalized CDF and generalized Probability Density Function (PDF) of a discrete random variable.

- the DET transition $\texttt{period}_{l,z}$ with value T_l and the DET transition $\texttt{offset}_{l,z}$ with value $O_{l,z}$ model the period and the offset, respectively, of the arrival process of trams at the wayside system;
- the GEN transition $\texttt{delay}_{l,z}$ with CDF $d_{l,z}$ models the tram delay on the nominal arrival time at the wayside system;
- the DET transition $\texttt{tLightTrigger}_{l,z}$ with value $G_{l,z}$ models the time needed by a tram to travel from the wayside system to the intersection;
- the GEN transition $\texttt{crossing}_{l,z}$ with CDF $c_{l,z}$ models the time spent by a tram in crossing the intersection.

The traffic light schedule submodel is a sequence of DET transitions $\texttt{phase}_1, \ldots, \texttt{phase}_W$ chained by their input places, where the value of $\texttt{phase}_w$ is the duration B_w of the wth phase $\forall\, w \in \{1, \ldots, W\}$, and the sum of the values of all transitions is equal to the traffic light period P.

The submodel of a vehicle flow represents a finite-capacity birth–death process where the birth rate is constant and the death rate may depend on the queue length. Specifically, the submodel of vehicle flow ϕ_i^{veh} consists of: $K_i + 1$ places $\texttt{Queue}_{i,0}, \ldots, \texttt{Queue}_{i,K_i}$ (where K_i is the queue capacity) modeling the condition that the queue contains $0, \ldots, K_i$ vehicles, respectively; K_i EXP transitions $\texttt{t}_{i,0}, \ldots, \texttt{t}_{i,K_i-1}$ with rate λ_i modeling a vehicle arrival; and, K_i EXP transitions $\texttt{s}_{i,0}, \ldots, \texttt{s}_{i,K_i-1}$ with rate $\mu_{i,0}, \ldots, \mu_{i,K_i-1}$, respectively, modeling a vehicle departure when the queue contains $1, \ldots, K_i$ vehicles, respectively. Each transition $\texttt{s}_{i,k}\ \forall\, k \in \{0, \ldots, K_i - 1\}$ has an enabling function that evaluates to true if the vehicle flow is allowed to cross the intersection according to the traffic light schedule (i.e., if the marking of the traffic light schedule submodel assigns one token to the input place of one of the transitions modeling the phases assigned to the vehicle flow) and if no tram of any track is approaching or crossing the intersection (i.e., if the marking of the submodel of each tram track $\phi_{l,z}^{\text{tram}}$ does not assign tokens to places $\texttt{TLightTrigger}_{l,z}$ and $\texttt{Crossing}_{l,z}$), e.g., if vehicle flow ϕ_i^{veh} crosses the tram tracks $\phi_{1,1}^{\text{tram}}$ and $\phi_{1,2}^{\text{tram}}$ and it is assigned the first phase Σ_1 (represented by transition $\texttt{phase}_1$), then the enabling function of transitions $\texttt{s}_{i,0}, \ldots, \texttt{s}_{i,K_i-1}$ evaluates to true if place $\texttt{Phase}_1$ contains one token and places $\texttt{TLightTrigger}_{1,1}$, $\texttt{TLightTrigger}_{1,2}$, $\texttt{Crossing}_{1,1}$, and $\texttt{Crossing}_{1,2}$ are empty. For simplicity of presentation, each queue state is explicitly represented by a dedicated place, though the submodel of vehicle flow ϕ_i^{veh} could be encoded in a more compact manner by: a place $\texttt{queue}_i$ whose marking represents the queue length; an EXP transition $\texttt{t}_i$ modeling vehicle arrivals, having rate λ_i, place $\texttt{queue}_i$ as an output place and an enabling function that evaluates to true if place $\texttt{queue}_i$ contains less than K_i tokens; and, an EXP transition $\texttt{t}_i$ modeling vehicle departures, having rate $\texttt{s}_i$ depending on the marking of place $\texttt{queue}_i$, and place $\texttt{queue}_i$ as an input place.

3. Problem formulation and solution

We evaluate the impact of tram lines on vehicle flows in terms of expected queue size, both in the transient phase up to a time limit, and in the long run. We use this result in Section 4.2 to derive the signal schedule that minimizes the maximum expected percentage of queued vehicles of each flow.

In principle, for each vehicle flow, the expected queue length over time could be derived through transient analysis of the STPN model of Fig. 3 based on the method of stochastic state classes [46], which enables quantitative evaluation of stochastic models where multiple non-EXP timers can be concurrently enabled in each state. However, this solution would not be practically feasible due to the high number of concurrent GEN transitions and the high number of firings to which GEN transitions remain persistent. This problem could not be circumvented even though the model size would be reduced by analyzing each vehicle flow submodel together only with the submodels that it depends on, i.e., the submodel of the traffic light schedule and the submodels of the tram tracks. Since the model includes multiple concurrently enabled DET and GEN transitions, solution methods that require at most one expolynomially distributed timer in each marking [52] could not be applied, and those that rely on the approximation of non-EXP transitions through phase-type distributions [53,54] would face significant complexity as well in approximating bounded supports. We recall that expolynomial functions, also termed exponomials [55], are defined as the sum of products of exponential and polynomial terms, i.e., $f(x) = \sum_{m=0}^{M-1} c_m \prod_{n=0}^{N-1} x_n^{\alpha_{mn}} e^{-\lambda_{mn} x_n}$.

Therefore, we propose an efficient compositional approach to decouple the analyses of tram lines and vehicle flows. On the one hand, each tram track submodel is analyzed in isolation by forward transient analysis based on the method of stochastic state classes to derive the transient probability that no tram is approaching or crossing the intersection, which we refer to as the *intersection availability* (Section 3.1). On the other hand, each vehicle flow submodel is translated into a *finite-capacity vacation queue* with EXP inter-arrival times, EXP service times, and *GEN vacation times* determined by the intersection availability [47–49] (Section 3.2). Transient queue behavior is defined by a set of ordinary differential equations constraining the conditional transient probabilities of queue lengths, whose solution yields the expected number of queued vehicles over time (Section 3.2.1).

While the expected queue length over time does not reach a steady state, due to the recurrent passages of trams and the periodic schedule of intersection traffic light, we prove that the distribution of the expected queue length reaches a steady state at multiples of the hyper-period, and we show that it can be derived by performing steady-state analysis of the DTMC embedded in the continuous-time birth–death process of the queue at multiples of the hyper-period (Section 3.2.2). Given that the steady-state distribution is experimentally observed to be reached within few hyper-periods, the expected queue size over time can be computed through transient analysis starting from the steady-state distribution up to the first hyper-period, enabling evaluation with time-varying stochastic parameters over intervals of arbitrary duration.

Table 2
CDFs of the transitions of the STPN submodels of tram tracks $\phi^{\text{tram}}_{1,1}$ and $\phi^{\text{tram}}_{1,2}$ of tram line ϕ^{tram}_{1} in Fig. 3 ($\text{UNIF}(a,b)$ denotes a uniform distribution over $[a,b]$; $\text{DET}(c)$ denotes the generalized distribution of a Dirac delta function centered at c).

Tram track $\phi^{\text{tram}}_{1,1}$		Tram track $\phi^{\text{tram}}_{1,2}$	
transition	CDF	transition	CDF
$\texttt{period}_{1,1}$	$\text{DET}(220\,\text{s})$	$\texttt{period}_{1,2}$	$\text{DET}(220\,\text{s})$
$\texttt{offset}_{1,1}$	$\text{DET}(0\,\text{s})$	$\texttt{offset}_{1,2}$	$\text{DET}(110\,\text{s})$
$\texttt{delay}_{1,1}$	$\text{UNIF}(0\,\text{s}, 120\,\text{s})$	$\texttt{delay}_{1,2}$	$\text{UNIF}(0\,\text{s}, 40\,\text{s})$
$\texttt{tLightTrigger}_{1,1}$	$\text{DET}(5\,\text{s})$	$\texttt{tLightTrigger}_{1,2}$	$\text{DET}(5\,\text{s})$
$\texttt{crossing}_{1,1}$	$\text{UNIF}(6\,\text{s}, 14\,\text{s})$	$\texttt{crossing}_{1,2}$	$\text{UNIF}(6\,\text{s}, 14\,\text{s})$

3.1. Evaluation of tram traffic behavior

The submodel of each tram track (see Fig. 3) can be evaluated by forward transient analysis based on the method of stochastic state classes [45,46] implemented by the ORIS tool [56] and the SIRIO library [57], which addresses models where multiple non-EXP timers can be concurrently enabled in each state (note that the DET transition modeling tram departures, e.g., $\texttt{period}_{1,1}$ in the submodel of tram track $\phi^{\text{tram}}_{1,1}$ shown in Fig. 3, is always enabled and at most one of the remaining transitions is also enabled). A stochastic state class encodes the current marking plus the joint support and the joint PDF of the elapsed time and the times-to-fire of the enabled transitions. The approach enumerates the stochastic state classes reached within a given time limit $t_{\max}$ and uses the probability that each class is the last node reached within $t \in [0, t_{\max}]$ to derive the probabilities of all markings at t. Thus, the probability $\alpha_{l,z}(t)$ that a tram of track $\phi^{\text{tram}}_{l,z}$ is neither approaching nor crossing the intersection at t can be derived as:

$$\alpha_{l,z}(t) = \sum_{m \in \mathcal{M}_{l,z}} p_m(t) \tag{1}$$

where $p_m(t)$ is the probability of marking m at time t and $\mathcal{M}_{l,z}$ is the set of markings where places $\texttt{trafficLightTrigger}_{l,z}$ and $\texttt{Crossing}_{l,z}$ are empty. Given that behaviors of trams of all tracks of all lines are independent of each other, the *intersection availability* $\alpha(t)$, i.e., the probability that no tram is either approaching or crossing the intersection at time t, can be computed as the product of probabilities $\alpha_{l,z}(t)$ of each tram track $\phi^{\text{tram}}_{l,z}$ of each tram line ϕ^{tram}_{l}, computed by Eq. (1):

$$\alpha(t) = \prod_{\substack{l \in \{1,\dots,L\} \\ z \in \{1,\dots,Z_l\}}} \alpha_{l,z}(t) \tag{2}$$

where L is the number of tram lines and Z_l is the number of tram tracks of tram line ϕ^{tram}_{l}.

Referring to the STPN model of Fig. 3, we consider an intersection between vehicle flow ϕ^{veh}_{1} and tram line ϕ^{tram}_{1} made of tracks $\phi^{\text{tram}}_{1,1}$ and $\phi^{\text{tram}}_{1,2}$. Table 2 shows the deterministic temporal parameters (i.e., always taking the same value) and stochastic temporal parameters (i.e., taking values according to a probability distribution) of the STPN submodels of the two tracks, derived by referring to a real scenario detected by the GEST company [58] for a critical intersection of the Florence tramway during a half-day of operation. On the one hand, deterministic temporal parameters are modeled by DET transitions. Specifically, in Fig. 3, the DET transitions $\texttt{period}_{1,1}$ and $\texttt{period}_{1,2}$ have value $T_1 = 220\,\text{s}$, which comprises the actual nominal inter-arrival time of trams during high-frequency hourly intervals; the DET transitions $\texttt{offset}_{1,1}$ and $\texttt{offset}_{1,2}$ have arbitrary values $O_{1,1} = 0\,\text{s}$ and $O_{1,2} = 110\,\text{s}$, respectively, selected not to synchronize tram passages and thus to illustrate the complexity of behaviors; and, the DET transitions $\texttt{trafficLightTrigger}_{1,1}$ and $\texttt{trafficLightTrigger}_{1,2}$ have value $G_{1,1} = G_{1,2} = 5\,\text{s}$, which is the actual advance on the tram arrival time with which traffic lights of vehicles are turned red.

On the other hand, without loss of generality, stochastic temporal parameters are modeled by GEN transitions with uniform CDF to facilitate the interpretability of results. Moreover, uniform CDFs are often advocated when measured data are not available and temporal parameters are described by a min–max duration but not by a probabilistic characterization [59], which might occur during early evaluation of design choices. In the specific case of the experiments reported in this paper, the GEN transition $\texttt{delay}_{1,1}$ is associated with a uniform CDF over $[0, 120]\,\text{s}$, where $120\,\text{s}$ is the maximum observed tram delay with respect to the nominal arrival time at the wayside system; the GEN transition $\texttt{delay}_{1,2}$ is arbitrarily associated with a uniform CDF over $[0, 40]\,\text{s}$ not to synchronize tram passages; and, the GEN transitions $\texttt{crossing}_{1,1}$ and $\texttt{crossing}_{1,2}$ are associated with a uniform CDF over $[6, 14]\,\text{s}$, where $6\,\text{s}$ and $14\,\text{s}$ are the minimum and maximum observed time needed by trams to cross the intersection, respectively. It is worth noting that the approach could encompass any GEN CDF in the class of expolynomial functions [55], with analytical representation over the entire domain or piecewise-defined over multiple sub-domains. Expolynomial CDFs are supported by the ORIS tool and the SIRIO and OMNIBUS libraries, affecting the complexity of the subsequent solution method only to a marginal extent, and facilitating fitting of statistics of duration data, which could be easily obtained from the tramway infrastructure [60,61].

Fig. 4 shows the transient probability $\alpha_{1,1}(t)$ that no tram of track $\phi^{\text{tram}}_{1,1}$ is either approaching or crossing the intersection (dashed line): $\alpha_{1,1}(t)$ decreases from time $0\,\text{s}$, i.e., the minimum time at which the tram may arrive at the wayside system, up to time $19\,\text{s}$, i.e., the maximum time at which the tram finishes crossing the intersection when it arrives at the wayside system at time $0\,\text{s}$; then, $\alpha_{1,1}(t)$ remains constant up to time $120\,\text{s}$, i.e., the maximum arrival time at the wayside system; finally, $\alpha_{1,1}(t)$ increases up to reaching

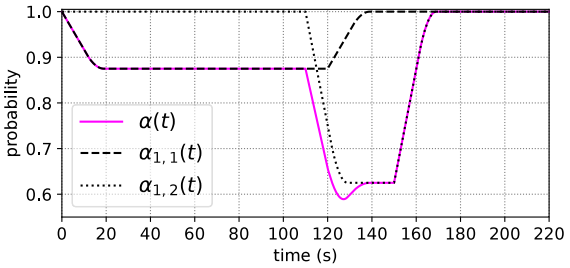

Fig. 4. For tram tracks $\phi_{1,1}^{\text{tram}}$ and $\phi_{1,2}^{\text{tram}}$ of the tram line ϕ_1^{tram} of Fig. 3, with the stochastic temporal parameters of Table 2, the plot shows the transient probability $\alpha_{1,1}(t)$ that no tram of track $\phi_{1,1}^{\text{tram}}$ is either approaching or crossing the intersection, the transient probability $\alpha_{1,2}(t)$ that no tram of track $\phi_{1,2}^{\text{tram}}$ is either approaching or crossing the intersection, and the transient probability $\alpha(t)$ that no tram of any of the two tracks is either approaching or crossing the intersection.

value 1 at time 139 s, i.e., the maximum time at which the tram leaves the intersection. Fig. 4 also shows the transient probability $\alpha_{1,2}(t)$ that no tram of track $\phi_{1,2}^{\text{tram}}$ is either approaching or crossing the intersection (dotted line): similarly, $\alpha_{1,2}(t)$ decreases from time 110 s (i.e., the minimum arrival time at the wayside system) up to time 129 s (i.e., the maximum time at which the tram finishes crossing the intersection when arriving at time 0 s at the wayside system), remains constant up to time 150 s (i.e., the maximum arrival time at the wayside system), and increases up to reaching value 1 at time 169 s (i.e., the maximum time at which the tram leaves the intersection). Fig. 4 also shows the transient probability $\alpha(t)$ that no tram of any of the two tracks is either approaching or crossing the intersection (fuchsia line), which is the product of $\alpha_{1,1}(t)$ and $\alpha_{1,2}(t)$ according to Eq. (2).

3.2. Evaluation of vehicle traffic behavior

Each vehicle flow is modeled as an *M/M finite-capacity vacation queue with GEN vacation time* [47], where vacations occur when the intersection is not available due to a tram passage or a signal red phase. Note that vacation durations and intertimes are both GEN, and service is *nonexhaustive* as vacations can start even when the queue is not empty. For instance, referring to the STPN model of Fig. 3, for an intersection between a single vehicle flow ϕ_1^{veh} and a tram line ϕ_1^{tram} made of a single track $\phi_{1,1}^{\text{tram}}$, the signal schedule defines a single phase assigned to ϕ_1^{veh}, and thus:

- the nth unavailability interval starts at a random time t_n following the GEN distribution of transition $\texttt{delay}_{1,1}$ shifted by the value $O_{1,1} + (n-1)\,T_1$ of the nominal arrival time of the nth tram at the wayside system, i.e., the distribution of t_n is $\text{UNIF}((n-1)\,220\,\text{s}, (n-1)\,220 + 120\,\text{s})$;
- the duration Δ_n of each unavailability interval follows the GEN distribution of transition $\texttt{crossing}_{1,1}$ shifted by the value $G_{1,1}$ of transition $\texttt{trafficLightTrigger}_{1,1}$, i.e., the distribution of Δ_n is $\text{UNIF}(11\,\text{s}, 19\,\text{s})$.

The queue may be modeled as a single server M/M/1/K vacation queue, where the intersection itself acts as the server, and the service time represents the time during which each vehicle is crossing the intersection. Alternatively, the queue may also be modeled as a multiple-server M/M/K/K vacation queue, to capture the fact that multiple vehicles drive along the road section before crossing the intersection, thus considering the overall road section as a set of servers and the rate of the Poisson process of vehicle departures as the rate of the time that queued vehicles take to advance one position in the queue. In doing so, the model still allows one vehicle at a time to leave the intersection, but it is able to better capture the process of vehicles approaching the intersection, which is not modeled at all by the M/M/1/K model.

A vast literature addresses the evaluation of *vacation* queueing systems considering both EXP and GEN vacation times [47,62,63], e.g., M/M/1 vacation queues with different service policies considered in [64], M/M/1 queues cyclically attended by the server in [65] according to various polling schemes with EXP walk time, and GI/M/c queues where servers take synchronous vacations with duration characterized by a phase type distribution [66]. *Markov modulated* queueing systems [67] are also investigated to model primary arrival or service processes controlled by a secondary Markov process, e.g., M/M/1 queues where the arrival and service rates depend on the state of a DTMC [67] or where the server speed is changed based on the measured utilization at decision points determined by a DTMC [68], queues characterized by a Markovian Arrival Process (MAP) [69] where arrivals are associated with state transitions of a hidden Continuous Time Markov Chain (CTMC), and MAP/M/c queues with phase-type vacation times [70,71]. In our model, the duration of server vacancy and the time between two consecutive starts of server vacancy have GEN distributions which are not explicitly given and are rather determined by a non-Markovian process, resulting from the composition of the marking processes underlying the STPN models of the tram tracks and the deterministic time-division multiplexing schedule of the intersection traffic light. According to this terminology, our models can be termed *non-Markov modulated vacation queueing systems*. Moreover, in our approach, control mechanisms to regulate the server speed are not considered, and the server may be unavailable with probability 1 during certain time intervals.

3.2.1. Evaluation of transient behavior

The submodel of vehicle flow ϕ_i^{veh} (as illustrated in Section 2.2 and Fig. 3) can be represented as an M/M/1/K_i vacation queue with GEN vacation time or as an M/M/K_i/K_i vacation queue with GEN vacation times, whose parameters are defined as illustrated in the following:

- The arrival rate is λ_i.
- The queue capacity is K_i.
- The number of servers is equal to 1 in the M/M/1/K_i queue, i.e., one vehicle at a time is allowed cross the intersection, and equal to the queue capacity K_i in the M/M/K_i/K_i queue.
- In the M/M/1/K_i queue, the service rate is $\mu_i \cdot \beta_i(t)\ \forall\, t \geqslant 0$, i.e., the rate μ_i of the EXP time that a vehicle takes to cross the intersection (when available), modulated by the probability $\beta_i(t)$ that ϕ_i^{veh} is allowed to cross the intersection at time t. In turn, given that the signal schedule is independent of tram passages, $\beta_i(t)$ can be derived as the product of the schedule $\sigma_i(t)$ of ϕ_i^{veh} (which equals 1 if t belongs to a phase assigned to ϕ_i^{veh} and 0 otherwise) and the intersection availability $\alpha(t)$ (i.e., probability that no tram is approaching or crossing the intersection at time t), i.e., $\beta_i(t) = \sigma_i(t) \cdot \alpha(t)\ \forall\, t \geqslant 0$.
  In the M/M/K_i/K_i queue, the service rate is $k \cdot \mu_i \cdot \beta_i(t)$ where k is the number of queued vehicles $\forall\, k \in \{0, 1, \dots, K_i\}$, i.e., the rate $k \cdot \mu_i$ of the EXP time that k vehicles take to leave the intersection (when available) and thus to advance one position in the queue, modulated by the probability $\beta_i(t)$ that ϕ_i^{veh} is allowed to cross the intersection at time t. Note that the service rate is linear in the queue length to facilitate interpretation of experimental results. Nevertheless, more complex functions could be considered, without affecting the complexity of the solution method to any extent.

To characterize the queue behavior, we compute the probability $R_{k,j}(t)$ that the number $Q(t)$ of queued vehicles at time t is equal to j given that the number $Q(0)$ of queued vehicles was equal to k at the initial time, $\forall\, k, j \in \{0, 1, \dots, K_i\}$, $\forall\, t > 0$, i.e., $R_{k,j}(t) := P\{Q(t) = j \mid Q(0) = k\}$. Specifically, $R_{k,j}(t)$ is characterized by a system of ordinary differential equations, obtained considering the system behavior during an infinitesimal time interval Δt tending to zero, so that the only transitions that may happen with non-negligible probability within that interval are one vehicle arrival (with probability $\lambda_i \Delta t$), or one vehicle departure (with probability $\mu_i \Delta t$), or neither arrivals nor departures (with probability $1 - \lambda_i \Delta t - \mu_i \Delta t$). According to this, for the M/M/1/K_i queue, $\forall\, k \in \{0, 1, \dots, K_i\}$, $\forall\, j \in \{1, \dots, K_i - 1\}$, and $\forall\, t \geqslant 0$, we obtain:

$$\begin{cases} R'_{k,0}(t) &= -\lambda_i R_{k,0}(t) + \mu_i \beta_i(t) R_{k,1}(t) \\ R'_{k,j}(t) &= -\lambda_i R_{k,j}(t) - \mu_i \beta_i(t) R_{k,j}(t) \\ & \quad + \lambda_i R_{k,j-1}(t) + \mu_i \beta_i(t) R_{k,j+1}(t) \\ R'_{k,K_i}(t) &= \lambda_i R_{k,K_i-1}(t) - \mu_i \beta_i(t) R_{k,K_i}(t) \end{cases} \tag{3}$$

where $R_{k,k}(0) := P\{Q(0) = k\}$ and $R_{k,j}(0) := P\{Q(0) = j \mid Q(0) = k\} = 0\ \forall\ k \neq j$. Similarly, for the M/M/K_i/K_i queue, $\forall\, k \in \{0, 1, \dots, K_i\}$, $\forall\, j \in \{1, \dots, K_i - 1\}$, and $\forall\, t \geqslant 0$, we obtain:

$$\begin{cases} R'_{k,0}(t) &= -\lambda_i R_{k,0}(t) + \mu_i \beta_i(t) R_{k,1}(t) \\ R'_{k,j}(t) &= -\lambda_i R_{k,j}(t) - j\mu_i \beta_i(t) R_{k,j}(t) \\ & \quad + \lambda_i R_{k,j-1}(t) + (j+1)\mu_i \beta_i(t) R_{k,j+1}(t) \\ R'_{k,K_i}(t) &= +\lambda_i R_{k,K_i-1}(t) - K_i \mu_i \beta_i(t) R_{k,K_i}(t) \end{cases} \tag{4}$$

Both Eqs. (3) and (4) can be numerically solved by discretization with time step δ over the interval $[0, t_{\max}]$, with linear complexity in the number $t_{\max}/\delta$ of time points and quadratic complexity in the queue capacity K_i. Note that the arrival process could be easily extended into a time-inhomogeneous Poisson Process by multiplying rate λ_i in Eq. (3) by a function of time, supporting representation of vehicles arriving in bursts, platoons and free flow. Similarly, both for arrival times and for leaving times, other non-EXP distributions could be easily considered that maintain the underlying stochastic process in the class of CTMCs, e.g., using hyper-EXP distributions and Markovian Arrival Processes.

For both queue models, the expected queue length $\bar{Q}(t)$ at time t can be derived by the total probability law, considering the initial distribution of the queue length, i.e., $R_{k,k}(0)\ \forall\, k \in \{0, 1, \dots, K_i\}$:

$$\bar{Q}(t) = \sum_{k=0}^{K_i} R_{k,k}(0) \sum_{j=0}^{K_i} j\, R_{k,j}(t) \tag{5}$$

Fig. 5(a) shows $\bar{Q}(t)$ for a vehicle flow with queue capacity $K = 31$ (derived from road section length $S = 150\,\text{m}$, vehicle length $C = 4.5\,\text{m}$, and safe distance $D = 0.3\,\text{m}$), arrival rate $\lambda = 0.9\,\text{s}^{-1}$, and leaving rate $\mu = 1.138\,\text{s}^{-1}$ for the M/M/1/K model (derived from maximum vehicle speed $V = 50\,\text{km h}^{-1}$ and intersection length $E = 12.2\,\text{m}$) and $\mu = 0.092\,\text{s}^{-1}$ for the M/M/K/K model (derived from maximum vehicle speed $V = 50\,\text{km h}^{-1}$ and road section length $S = 150\,\text{m}$), which intersects a tram line with two tracks, each modeled by the tram track submodel of Fig. 3 considering the stochastic parameters of Table 2. Specifically, $\bar{Q}(t)$ is computed by solving the systems of Eqs. (3) and (4) up to time 660 s (i.e., 3 hyper-periods, each having duration $H = 220\,\text{s}$) with time step 0.1 s, considering that the queue is empty at the initial time, i.e., the initial distribution is $R_{0,0}(0) = 1$ and $R_{k,k}(0) = 0\ \forall\, k \in \{1, \dots, K_i\}$. As expected, due to the recurrent passages of trams, $\bar{Q}(t)$ soon reaches an almost periodic pattern for both the M/M/1/K model and the M/M/K/K model (except during an initial small transitory interval), with peaks and troughs corresponding to low and high values of the intersection availability $\alpha(t)$ shown in Fig. 4. With respect to the M/M/1/K curve, the M/M/K/K curve shows increasing

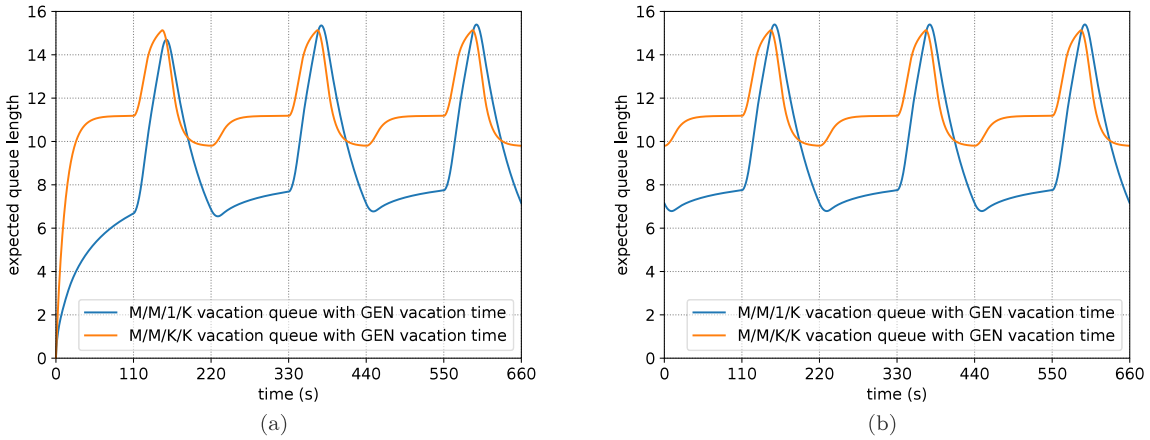

Fig. 5. Transient expected queue length evaluated on the M/M/1/K and M/M/K/K models from the initial condition of an empty queue (a) and from a queue with a random number of vehicles distributed according to the steady state distribution (b).

and decreasing sections slightly shifted to the left and with slightly lower peaks and higher troughs. These effects are due to the fact that, in the M/M/K/K model, all the vehicles queued in the road section are considered to be served (instead of only the one crossing the intersection), which makes the queue fill and empty earlier, and the peak-to-trough amplitude be lower.

3.2.2. Evaluation of steady-state behavior

We prove existence and we derive the steady-state distribution of the number of queued vehicles at multiples of the hyper-period. To this end: (1) first, we derive the transition probability matrix of the DTMC $\mathbb{X}$ embedded in the continuous-time birth death process $\mathbb{Y}$ of the queue (i.e., either the M/M/1/K_i queue or the M/M/K_i/K_i queue), by performing transient analysis of the queue behavior within a hyper-period (i.e., by solving the set of ordinary differential equations of either Eq. (3) or Eq. (4), respectively); (2) then, we prove that the DTMC $\mathbb{X}$ is irreducible, aperiodic, and positive recurrent; and, (3) finally, we prove that there exists a unique steady-state distribution of the number of queued vehicles at multiples of the hyper-period and we derive it through steady-state analysis of the DTMC $\mathbb{X}$.

1. The DTMC $\mathbb{X}$ consists of $K_i + 1$ states $s_0, s_1, \ldots, s_{K_i}$ modeling the number $0, 1, \ldots, K_i$ of queued vehicles, respectively, and $(K_i + 1)^2$ transitions between any pair of states $\langle s_k, s_j \rangle \ \forall\, k, j \in \{0, 1, \ldots, K_i\}$. Note that $P\{Q((n+1)H) = j \mid Q(nH) = k\} = P\{Q(H) = j \mid Q(0) = k\}$, given that $\mathbb{Y}$ has constant birth rate λ_i and periodic death rate with period H, either $\mu_i\, \beta_i(t)$ for the M/M/1/K_i model or $k\, \mu_i\, \beta_i(t)$ for the M/M/K_i/K_i model. Therefore, the transition probability from state s_k to state s_j of $\mathbb{X}$ is defined as $P_{k,j} := P\{Q(H) = j \mid Q(0) = k\} = R_{k,j}(H)\ \forall\, k, j \in \{0, 1, \ldots, K_i\}$. According to this, solution of the system of Eq. (3) or Eq. (4) within $[0, H]$ for the M/M/1/K_i queue and the M/M/K_i/K_i queue, respectively, is sufficient to compute the transition probability matrix $\boldsymbol{P}$ of $\mathbb{X}$.
2. By definition, any state of the birth–death process $\mathbb{Y}$ can be reached from any other state after a non-null time, and thus after a hyper-period, i.e., $R_{k,j}(H) > 0\ \forall\, k, j \in \{0, 1, \ldots, K_i\}$. According to this, the DTMC $\mathbb{X}$ is irreducible (i.e., any state can be reached from any other state) and aperiodic (i.e., any return to a state can occur in any number of steps). Given that $\mathbb{X}$ is irreducible and has finite state space, $\mathbb{X}$ is also positive recurrent (i.e., the mean return time to each state is finite).
3. Since $\mathbb{X}$ is irreducible, aperiodic, and positive recurrent, the limiting probability $\pi_k := \lim_{n->\infty} p_k(n)$ exists $\forall\, k \in \{0, 1, \ldots, K_i\}$, where $p_k(n) := P\{Q(nH) = k\}$ is the probability of k queued vehicles at the beginning of the $(n+1)$th hyper-period. The row vector $\boldsymbol{\pi} := \{\pi_0, \pi_1, \ldots, \pi_{K_i}\}$ of the limiting probabilities is independent of the initial probability distribution $\boldsymbol{p}(0) := \{p_0(0), p_1(0), \ldots, p_{K_i}(0)\}$, is the unique steady-state probability distribution, and can be computed by solving the following system of linear equations, where $\boldsymbol{P}$ is the transition probability matrix of $\mathbb{X}$:

$$\begin{cases} \boldsymbol{\pi} = \boldsymbol{\pi}\, \boldsymbol{P} \\ |\boldsymbol{\pi}| = 1 \end{cases} \tag{6}$$

We solve Eq. (6) numerically by the Successive Over Relaxation (SOR) iterative method [72], with quadratic complexity in the number of states of $\mathbb{X}$.

Figs. 6(a) and 6(b) plot the steady-state distribution of the queue length at multiples of the hyper-period, computed through the M/M/1/K_i and the M/M/K_i/K_i vacation queue with GEN vacation time, respectively, for the intersection analyzed in Fig. 5. The steady-state distribution computed through the M/M/1/K_i model has expected value (i.e., 7.151) lower than the one obtained through the M/M/K_i/K_i model (i.e., 9.801), as suggested by the expected number of queued vehicles over time plotted in Fig. 5(a), where peaks of the M/M/K_i/K_i curve are slightly lower than those of the M/M/1/K_i curve, while troughs are significantly higher. Fig. 5(b) plots the expected number of queued vehicles over time computed for both models assuming initial distribution of the

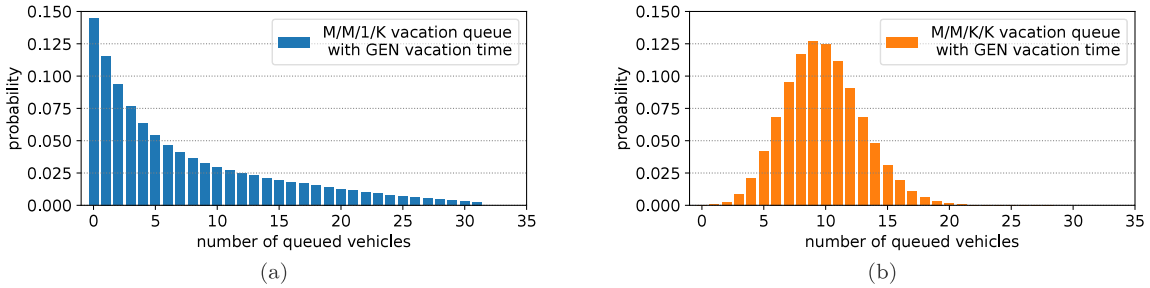

Fig. 6. Steady-state distribution of the number of queued vehicles at multiples of the hyper-period for the intersection analyzed in Fig. 5, computed through: (a) the M/M/1/K and (b) the M/M/K/K vacation queue with GEN vacation time.

number of queued vehicles equal to the corresponding steady-state distribution at multiples of the hyper-period. With respect to the curves of Fig. 5(a), derived assuming that the queue is empty at the initial time, the pattern is exactly periodic with period equal to the hyper-period $H = 220\,\text{s}$.

3.2.3. Remarks

According to the above treatment, given the values of the system parameters (i.e., the parameters of the intersection, vehicle flows, and tram lines), variability over time of the expected queue length of each vehicle flow is captured in the vehicle flow submodel by modulating the queue service rate according to the probability over time that the vehicle flow is allowed to cross the intersection, which, in turn, is determined by the synchronous passages of trams and the deterministic schedule of the intersection traffic light. In particular, the evaluation of the expected queue length over time of each vehicle flow can be performed by transient analysis of the queue behavior, as illustrated in Section 3.2.1. When the values of the system parameters vary over multiple time slots (e.g., due to daily time patterns), variability of the expected queue length of each vehicle flow from one time slot to the next one is captured by performing, for each time slot, transient analysis of the queue behavior up to the first hyper-period, starting from the steady-state distribution (of the queue length at multiples of the hyper-period) reached within the previous time slot, as illustrated in Section 3.2.2. In doing so, by combining transient and steady-state analyses, the proposed approach enables evaluation of the expected queue length of each vehicle flow over time intervals that have arbitrary duration and under parameter values that vary over time.

4. Experimental evaluation

We assess feasibility and effectiveness of the approach comparing with simulation based on the SUMO tool [44]. As an instrumental step, we compare the expected queue length over time, derived through the M/M/1/K and the M/M/K/K model variants, in the case of an intersection between a vehicle flow and a bidirectional tram line (i.e., tram line made of two tracks having same tram departure period), which shows that the M/M/K/K model provides a better fit of values obtained with SUMO simulation (Section 4.1). We thus leverage the M/M/K/K model to derive optimal signal schedules that minimize the maximum expected percentage of queued vehicles of each flow, showing that the approach is able to identify the optimal schedule for intersections of real complexity while reducing computation time by nearly four orders of magnitude with respect to SUMO (Section 4.2).

The approach is implemented in the novel Java library OMNIBUS, which provides a Domain Specific extension of the SIRIO library [57] of the ORIS tool [56] to represent STPN models and to perform forward transient analysis of STPN models and steady-state analysis of DTMCs in the framework of the proposed approach. OMNIBUS is released with this paper, under AGPLv3 licence, and it is made available for replication of results and reuse at https://doi.org/10.5281/zenodo.10693840. A repository supporting comparison of experimental results against those obtained with SUMO is available at https://doi.org/10.5281/zenodo.10695718, under the EPLv2 licence. Experiments are performed on an Intel Core i5-6400 processor with 2.70 GHz frequency and 16 GB RAM.

4.1. Comparison between the M/M/1/K and the M/M/K/K vacation queues with GEN vacation time

We consider an intersection where a bidirectional tram line has priority over a single-lane vehicle flow. We consider the following parameter values, also summarized in Table 3 (note that parameters of the traffic light schedule are not shown given that a single vehicle flow is considered):

- The intersection has the typical length $E = 12.2\,\text{m}$ of an intersection in SUMO.
- Tram tracks have the stochastic parameters of Table 2, except for the offset of the second track which is $40\,\text{s}$ instead of $110\,\text{s}$. Specifically: trams of both tracks have arrival period $T = 220\,\text{s}$, travel time from the wayside system to the intersection equal to $5\,\text{s}$, and crossing time uniformly distributed over $[6, 14]\,\text{s}$; the offset O of tram arrivals is null for the first track and equal to $40\,\text{s}$ for the second one; and, the delay with respect to the nominal arrival time at the wayside system is uniformly distributed over $[0, 120]\,\text{s}$ for the first track and $[0, 40]\,\text{s}$ for the second one. Note that these parameter values tend to synchronize tram

Table 3
Parameters used in the comparison between the M/M/1/K and the M/M/K/K models.

	intersection parameter	values
E	intersection length	12.2 m
	vehicle flow ϕ_1^{veh} parameter	**value**
S	road section length	$\{50, 150, 450\}$ m
C	vehicle length	4.5 m
D	minimum vehicle distance	0.3 m
V	maximum vehicle speed	$\{30, 50, 70\}$ km h^{-1}
K	vehicle queue capacity	$\{10, 31, 93\}$
ρ	initial queue length distribution	$R_{0,0}(0) = 1$ and $R_{k,k}(0) = 0\ \forall k \in \{1, 2, \ldots, K\}$ (empty queue)
λ	vehicle arrival rate	$\{0.5, 0.9, 1.3\}$ s^{-1}
μ_{MM1K}	vehicle leaving rate in the M/M/1/K model	$\{0.683, 1.138, 1.593\}$ s^{-1}
μ_{MMKK}	vehicle leaving rate in the M/M/K/K model	$\{0.166, 0.277, 0.388, 0.055, 0.0920.129, 0.018, 0.030, 0.043\}$ s^{-1}
	tram line ϕ_1^{tram} parameter	**value**
T	period	220 s
	tram track $\phi_{1,1}^{\text{tram}}$ parameter	**value**
$O_{l,z}$	offset	0 s
$d_{l,z}$	delay distribution	UNIF(0 s, 120 s)
$G_{l,z}$	red signal trigger time	5 s
$c_{l,z}$	crossing time distribution	UNIF(6 s, 14 s)
	tram track $\phi_{1,2}^{\text{tram}}$ parameter	**value**
$O_{l,z}$	offset	40 s
$d_{l,z}$	delay distribution	UNIF(0 s, 40 s)
$G_{l,z}$	red signal trigger time	5 s
$c_{l,z}$	crossing time distribution	UNIF(6 s, 14 s)

passages, and thus to increase duration of the intervals of intersection unavailability, making search for optimal schedules more challenging. In particular, the intersection availability takes minimum value nearly equal to 0.547, and keeps this value in the entire range $[59, 80]$ s. Thus, the expected queue size over time exhibits peaks around 80 s (see Fig. 7). Conversely, in Fig. 4, the intersection availability takes minimum value nearly equal to 0.589, and keeps this value in the much smaller interval $[126.7, 127.7]$ s.

- The road section that precedes the intersection has length $S \in \{50, 150, 450\}$ m, and vehicles have length $C = 4.5$ m and safe distance $D = 0.3$ m, thus yielding queue capacity $K \in \{10, 31, 93\}$. Vehicles have maximum allowed speed $V \in \{30, 50, 70\}$ km h^{-1} and arrival rate $\lambda \in \{0.5, 0.9, 1.3\}$ s^{-1}. In the OMNIBUS model, for the M/M/1/K queue, the rate μ_{MM1K} of the time a vehicle takes to leave the intersection is equal to V/E, thus yielding $\mu_{\text{MM1K}} \in \{0.683, 1.138, 1.593\}$ s^{-1}; conversely, for the M/M/K/K queue, the rate μ_{MMKK} of the time a vehicle takes to advance one position in the queue is equal to V/S, thus yielding $\mu_{\text{MMKK}} \in \{0.166, 0.277, 0.388, 0.055, 0.0920.129, 0.018, 0.030, 0.043\}$ s^{-1}. Moreover, in the SUMO model, the reaction mode of drivers can be either normal or fast according to the default car following model implemented in SUMO, i.e., a variant of the Krauss model [73] where vehicles drive as fast as possible while maintaining perfect safety; and, the arrival policy of vehicles when the queue is full can be either leave (i.e., abandoning the road section) or queue (i.e., entering the road section as soon as the line runs).

This scenario is implemented in the OMNIBUS library and the SUMO simulator for each of the 27 cases resulting from the combination of values of S, λ, and V. Notably, both the OMNIBUS model (i.e., the STPN submodels of tram tracks and the queue modeling vehicle traffic) and the SUMO model can be derived, in principle automatically, from the metamodel of Fig. 1.

We evaluate the expected queue length $\bar{Q}(t)$ over an interval with duration equal to 5 hyper-periods, i.e., $[0, 5H]$, with hyper-period $H = 220$ s and time step $\delta = 0.1$ s, considering that the queue is empty at the initial time, i.e., $R_{0,0}(0) = 1$ and $R_{k,k}(0) = 0$ $\forall k \in \{1, 2, \ldots, K\}$. Then, we evaluate the error committed over the interval $[2H, 5H]$ by the analysis of the OMNIBUS model (with both the M/M/1/K and the M/M/K/K queue) with respect to a ground truth obtained by simulation of the SUMO model. Specifically, we compute the Normalized Root Mean Square Deviation (NRMSD):

$$\text{NRMSD(A, S)} := \sqrt{\frac{\sum_{t=0}^{N-1} (\bar{Q}_{\text{A}}(t) - \bar{Q}_{\text{S}}(t))^2}{N}} \cdot \frac{1}{K} \tag{7}$$

where $\bar{Q}_{\text{A}}(t)$ and $\bar{Q}_{\text{S}}(t)$ are the expected number of queued vehicles at time t computed by the analysis and simulation, respectively, and N is the number of time points, i.e., $N := 3H/\delta + 1$. Notes that normalization by the queue capacity K facilitates the comparison among scenarios with different scale, e.g., $K = 10$ with $S = 50$ m, while $K = 93$ with $S = 450$ m.

4.1.1. Derivation of ground truth through SUMO

In SUMO, the tram track model is implemented using a road section of length 25 m to represent the distance between the wayside system and an intersection of length E. Trams enter each track with maximum speed equal to 18 km h^{-1} (so that traveling 25 m takes

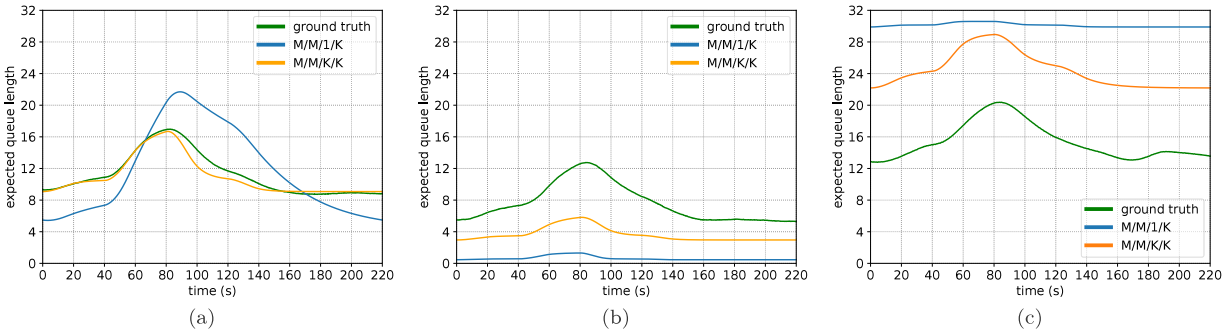

Fig. 7. Expected number of queued vehicles for the scenarios of Table 4 with: (a) $S = 150\,\text{m}$, $\lambda = 1.3\,\text{s}^{-1}$, and $V = 70\,\text{km}\,\text{h}^{-1}$; (b) $S = 150\,\text{m}$, $\lambda = 0.5\,\text{s}^{-1}$, and $V = 70\,\text{km}\,\text{h}^{-1}$; and, (c) $S = 150\,\text{m}$, $\lambda = 1.3\,\text{s}^{-1}$, and $V = 30\,\text{km}\,\text{h}^{-1}$.

nearly 5 s) and inter-arrival time equal to the period T plus the offset O plus the accumulated delay sampled from the a uniform distribution, over $[0, 120]$ s for the first track and over $[0, 40]$ s for the second one. When a tram arrives at the wayside system, the vehicle traffic light is turned and maintained red for a time equal to 5 s, needed by the tram to travel from the wayside system to the intersection, plus a time sampled from a uniform distribution over $[6, 14]$ s, needed by the tram to cross the intersection.

In SUMO, the vehicle flow model is implemented using a street of length S preceding an intersection of length E, with vehicles of length C maintaining safe distance D and maximum speed V. Given that SUMO prevents the inter-arrival time of vehicles to be too small, in the experiments we consider largest arrival rate equal to $1.5\,\text{s}^{-1}$, corresponding to minimum inter-arrival time equal to $\gamma = 0.66$ s. If the arrival rate in the STPN model is λ, then, in SUMO simulations, inter-arrival times of vehicles are equal to γ plus a time sampled from an EXP distribution with rate $\lambda' = 1/(1/\lambda - \gamma)$, so that the inter-arrival time has still mean $1/\lambda$ but it is not lower than γ. Moreover, preliminary experimental results show that the accuracy attained by the proposed approach in evaluating the expected number of queued vehicles over time is not affected by the reaction mode of drivers (which can be either normal or fast) and by the arrival policy with full queue (which can be either leave or queue, in the latter case letting vehicles enter the street as soon as the line runs). Therefore, in the experiments, the reaction mode of drivers is set to normal, and the arrivals of vehicles are discarded if the queue is full.

To determine the number of simulation runs, we consider the case with $S = 150\,\text{m}$, $\lambda = 0.9\,\text{s}^{-1}$, and $V = 50\,\text{km}\,\text{h}^{-1}$, we perform simulation up to time $5\,H = 1100\,\text{s} \simeq 18.3\,\text{min}$ with time step 0.1 s, and we progressively increase the number n of runs by 25 at a time, computing the NRMSD achieved by the n-run simulation with respect to the $(n + 25)$-run simulation. Results show that the NRMSD is in the order of $0.5 \cdot 10^{-3}$ after 1000 runs, lower than 10^{-3} after 1400 runs, and lower than 10^{-4} after 15 000 runs. Given that 1000 runs take nearly 7 h on average, and that NRMSD lower than 10^{-3} is sufficient for the context of use, we perform 1500 runs for each of the 27 cases, requiring a total execution time of nearly 11 days. Conversely, analysis is much faster than even a simulation run, requiring less than 2.7 s for each scenario, i.e., less than 1 s to perform forward transient analysis of the STPN of each tram track and less than 650 ms to perform transient and steady-state analysis of the vehicle queue. Note that, to achieve NRMSD equal to that obtained by the analysis with the M/M/K/K queue (i.e., 0.068, see Table 4 in Section 4.1.2), 3 simulation runs are needed requiring nearly 1.5 min, which is more than one order of magnitude larger than the analysis time. In practice, a few dozen of runs are still necessary to obtain sufficiently smooth curves without resorting to interpolation, especially for more complex scenarios with multiple vehicle flows.

4.1.2. Experimental results

For each considered scenario, Table 4 reports the NRMSD (computed by Eq. (7)) achieved by the analysis with respect to the ground truth in the evaluation of the expected number of queued vehicles over time. Specifically, the analysis exploiting the M/M/K/K queue achieves NRMSD lower than 0.37 in the worst case, lower than 0.2 in more than 80% of the cases, lower than 0.1 in nearly half of the cases, and equal to 0.022 in the best case, outperforming the analysis exploiting the M/M/1/K queue, which achieves NRMSD equal to 0.576 in the worst case, between 0.3 and 0.576 in one third of the cases, lower than 0.2 in nearly 22% of the cases, lower than 0.1 in nearly 11% of the cases, and equal to 0.058 in the best case.

For any street length, the analysis with the M/M/K/K queue tends to underestimate the expected number of queued vehicles if the arrival rate is low (which can be ascribed to the fact that the multiple-server semantics does not accurately capture single-vehicle dynamics), to overestimate it if the arrival rate is high (which can be due to the fact that EXP leaving times corresponding to medium speed overestimate actual leaving times, and due to the fact that this phenomenon seems to become observable in terms of queue size when the number of vehicles is high), and to be quite accurate otherwise. In all cases, increasing the maximum vehicle speed tends to decrease the computed metrics (which can be ascribed to the fact that EXP leaving times corresponding to high speed actually underestimate actual leaving times), thus improving overestimates and worsening underestimates. Fig. 7(a) plots the expected number of queued vehicles for the case with the lowest NRMSD, i.e., the case with $S = 150\,\text{m}$, $\lambda = 1.3\,\text{s}^{-1}$, and $V = 70\,\text{km}\,\text{h}^{-1}$, showing a trend very close to the ground truth. As already discussed, reducing the arrival rate to $\lambda = 0.5\,\text{s}^{-1}$ yields an underestimate (see Fig. 7(b)), while reducing the maximum vehicle speed to $V = 30\,\text{km}\,\text{h}^{-1}$ yields an overestimate (see Fig. 7(c)).

Table 4
Accuracy (NRMDS) of the analysis with the M/M/1/K and M/M/K/K queue with respect to SUMO ground truth, for 27 scenarios resulting from the combinations of values of: *i*) the street length S, which determines the queue capacity K; *ii*) the vehicle arrival rate λ; and, *iii*) the maximum vehicle speed V, which determines the leaving time rates μ_{MM1K} and (together with S) μ_{MMKK}. Best and worst NRMSD values are highlighted with gray background.

S (m)	K	λ (s^{-1})	V ($km\,h^{-1}$)	$\mu_{\text{MM1}K}$ (s^{-1})	$\mu_{\text{MM}K\text{K}}$ (s^{-1})	NRMSD($A_{\text{MM1}K}, S$)	NRMSD($A_{\text{MM}K\text{K}}, S$)
50	10	0.5	30	0.683	0.166	0.093	0.170
			50	1.138	0.277	0.233	0.212
			70	1.593	0.388	0.238	0.207
		0.9	30	0.683	0.166	0.270	0.025
			50	1.138	0.277	0.076	0.174
			70	1.593	0.388	0.224	0.238
		1.3	30	0.683	0.166	0.382	0.154
			50	1.138	0.277	0.255	0.026
			70	1.593	0.388	0.058	0.127
150	31	0.5	30	0.683	0.055	0.223	0.105
			50	1.138	0.092	0.281	0.145
			70	1.593	0.129	0.234	0.136
		0.9	30	0.683	0.055	0.439	0.089
			50	1.138	0.092	0.123	0.068
			70	1.593	0.129	0.286	0.135
		1.3	30	0.683	0.055	0.482	0.293
			50	1.138	0.092	0.469	0.100
			70	1.593	0.129	0.121	0.022
450	93	0.5	30	0.683	0.018	0.342	0.076
			50	1.138	0.030	0.272	0.087
			70	1.593	0.043	0.203	0.074
		0.9	30	0.683	0.018	0.489	0.122
			50	1.138	0.030	0.256	0.025
			70	1.593	0.043	0.300	0.076
		1.3	30	0.683	0.018	0.504	0.364
			50	1.138	0.030	0.576	0.150
			70	1.593	0.043	0.137	0.049

The same trends are exacerbated for the analysis with the M/M/1/K queue, especially with medium and large street length. Overall, the analysis with the M/M/K/K queue provides results that reproduce the ground truth pattern with sufficient accuracy for the context of use, capturing peaks and troughs of the expected number $\bar{Q}_{\text{S}}(t)$ of queued vehicles over time provided by the SUMO ground truth, and appearing open to improvements through the refinement of the analytical form of the service rate dependent on the queue size. Notably, the expected number $\bar{Q}_{\text{A}}(t)$ of queued vehicles over time computed by the analysis is able to capture relative variations of $\bar{Q}_{\text{S}}(t)$ as the values of parameters change, e.g., both $\bar{Q}_{\text{S}}(t)$ and $\bar{Q}_{\text{A}}(t)$ decrease as the arrival rate λ decreases, and they both increase as the maximum vehicle speed V decreases. Thus, thanks also to the significantly lower computational load with respect to SUMO, the approach can be exploited to derive the values of system parameters that optimize quantitative measures of interest concerned with the expected occupancy state of the queue of each vehicle flow.

4.2. Derivation of optimal signal schedules

We consider the urban intersection of Fig. 8 where three independent vehicle flows cross a bidirectional tram line, we define a space of schedules for the traffic lights of the three vehicle flows, and we show that the proposed approach can be used to derive a schedule that minimizes the maximum expected percentage of queued vehicles of each flow, considering different values of the arrival rates and the maximum speed of vehicles and comparing the obtained results with those computed through SUMO (Section 4.2.1). Then, we consider 4 time intervals and we vary both the period of tram departures and the arrival rate of each vehicle flow within each time interval, and we illustrate how the approach can be used to derive optimal signal schedules for each time interval (Section 4.2.2). In each time interval, we leverage the model of the M/M/K/K vacation queue with GEN vacation time, performing transient analysis starting from the steady-state distribution of the number of queued vehicles at multiples of the hyper-period reached within the previous time interval (except for the first time interval, for which the analysis of each flow is started from empty queue).

4.2.1. Validation with respect to SUMO

We consider an intersection among a bidirectional tram line having the parameter values considered in Section 4.1 and three vehicle flows ϕ_1^{veh}, ϕ_2^{veh}, and ϕ_3^{veh} with arrival rate $\lambda_1 = 0.05\,s^{-1}$, $\lambda_2 = 0.1\,s^{-1}$, and $\lambda_3 = 0.15\,s^{-1}$, respectively, queue capacity $K = 31$ (derived from street length $S = 150\,m$, vehicle length $C = 4.5\,m$, and safe distance $D = 0.3\,m$), and leaving rate $\mu = 0.092\,s^{-1}$ (derived from S and the maximum speed $V = 50\,km\,h^{-1}$). Fig. 8 shows a graphical representation of the intersection.

We consider the set of traffic signal schedules built as follows, resulting in 390 different schedules: (*i*) we consider period $P = 110\,s$ (i.e., half of the period $T = 220\,s$ of tram departures) and phases of duration $\Delta \in \{15, 25, 35\}$ s (except for the last phase which may be longer); (*ii*) we place a short time interval of 5 s during which all vehicle signals are red between any two phases assigned to

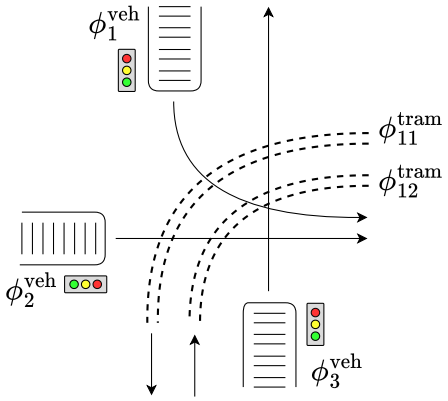

Fig. 8. A graphical representation of an intersection among three vehicle flows and a bidirectional tram line.

Table 5
For the intersection of Fig. 8 with arrival rates $\lambda_1 = 0.05\,\text{s}^{-1}$, $\lambda_2 = 0.1\,\text{s}^{-1}$, and $\lambda_3 = 0.15\,\text{s}^{-1}$ for vehicle flows ϕ_1^{veh}, ϕ_2^{veh}, and ϕ_3^{veh}, respectively, and with maximum vehicle speed $V = 50\,\text{km}\,\text{h}^{-1}$, the best 10 schedules, the median 3 schedules, and the worst 3 schedules in terms of maximum expected percentage $\bar{q}_{\text{A}}^{\max}$ of queue occupation of any flow computed by our analysis, the maximum expected percentage $\bar{q}_{\text{S}}^{\max}$ of queue occupation of any flow computed by SUMO simulation (25 runs), and the corresponding rank position.

Analysis rank position	$\bar{q}_{\text{A}}^{\max}$	SUMO rank position	$\bar{q}_{\text{S}}^{\max}$
$\sigma_1 := \langle(\phi_2^{\text{veh}}, 15), (\phi_3^{\text{veh}}, 25), (\phi_2^{\text{veh}}, 15), (\phi_1^{\text{veh}}, 15), (\phi_3^{\text{veh}}, 15)\rangle$	0.301	1	0.297
$\sigma_2 := \langle(\phi_2^{\text{veh}}, 15), (\phi_3^{\text{veh}}, 25), (\phi_1^{\text{veh}}, 15), (\phi_2^{\text{veh}}, 15), (\phi_3^{\text{veh}}, 15)\rangle$	0.301	4	0.308
$\sigma_3 := \langle(\phi_3^{\text{veh}}, 25), (\phi_2^{\text{veh}}, 15), (\phi_1^{\text{veh}}, 15), (\phi_3^{\text{veh}}, 15), (\phi_2^{\text{veh}}, 15)\rangle$	0.306	11	0.326
$\sigma_4 := \langle(\phi_3^{\text{veh}}, 25), (\phi_1^{\text{veh}}, 15), (\phi_2^{\text{veh}}, 15), (\phi_3^{\text{veh}}, 15), (\phi_2^{\text{veh}}, 15)\rangle$	0.306	27	0.357
$\sigma_5 := \langle(\phi_2^{\text{veh}}, 35), (\phi_3^{\text{veh}}, 15), (\phi_1^{\text{veh}}, 15), (\phi_3^{\text{veh}}, 25)\rangle$	0.316	9	0.320
$\sigma_6 := \langle(\phi_1^{\text{veh}}, 15), (\phi_2^{\text{veh}}, 15), (\phi_3^{\text{veh}}, 15), (\phi_2^{\text{veh}}, 15), (\phi_3^{\text{veh}}, 25)\rangle$	0.316	5	0.310
$\sigma_7 := \langle(\phi_1^{\text{veh}}, 15), (\phi_2^{\text{veh}}, 15), (\phi_3^{\text{veh}}, 15), (\phi_2^{\text{veh}}, 15), (\phi_3^{\text{veh}}, 25)\rangle$	0.316	10	0.325
$\sigma_8 := \langle(\phi_2^{\text{veh}}, 15), (\phi_3^{\text{veh}}, 15), (\phi_2^{\text{veh}}, 15), (\phi_1^{\text{veh}}, 15), (\phi_3^{\text{veh}}, 25)\rangle$	0.318	6	0.315
$\sigma_9 := \langle(\phi_2^{\text{veh}}, 15), (\phi_3^{\text{veh}}, 15), (\phi_1^{\text{veh}}, 15), (\phi_2^{\text{veh}}, 15), (\phi_3^{\text{veh}}, 25)\rangle$	0.318	2	0.303
$\sigma_{10} := \langle(\phi_3^{\text{veh}}, 25), (\phi_2^{\text{veh}}, 35), (\phi_3^{\text{veh}}, 15), (\phi_1^{\text{veh}}, 15)\rangle$	0.319	14	0.338
...	...	...	...
$\sigma_{194} := \langle(\phi_2^{\text{veh}}, 25), (\phi_1^{\text{veh}}, 15), (\phi_3^{\text{veh}}, 35), (\phi_1^{\text{veh}}, 15)\rangle$	0.509	126	0.521
$\sigma_{195} := \langle(\phi_1^{\text{veh}}, 25), (\phi_2^{\text{veh}}, 15), (\phi_3^{\text{veh}}, 35), (\phi_2^{\text{veh}}, 15)\rangle$	0.509	132	0.556
$\sigma_{196} := \langle(\phi_3^{\text{veh}}, 25), (\phi_1^{\text{veh}}, 25), (\phi_2^{\text{veh}}, 25), (\phi_1^{\text{veh}}, 15)\rangle$	0.525	159	0.613
...	...	...	...
$\sigma_{388} := \langle(\phi_1^{\text{veh}}, 15), (\phi_2^{\text{veh}}, 15), (\phi_1^{\text{veh}}, 15), (\phi_3^{\text{veh}}, 15), (\phi_2^{\text{veh}}, 25)\rangle$	0.822	379	1.0
$\sigma_{389} := \langle(\phi_2^{\text{veh}}, 15), (\phi_1^{\text{veh}}, 15), (\phi_2^{\text{veh}}, 15), (\phi_3^{\text{veh}}, 15), (\phi_1^{\text{veh}}, 25)\rangle$	0.822	334	1.0
$\sigma_{390} := \langle(\phi_2^{\text{veh}}, 25), (\phi_1^{\text{veh}}, 25), (\phi_3^{\text{veh}}, 15), (\phi_2^{\text{veh}}, 25)\rangle$	0.822	390	1.0

vehicle flows; and, (*iii*) in case the last phase lasted less than 15 s, we assign the time until the end of the period to the second-to-last phase (to guarantee that each phase has duration at least equal to 15 s). For instance, within each period $[0, 110]$ s, the schedule $\langle(\phi_1^{\text{veh}}, 35), (\cdot, 5), (\phi_2^{\text{veh}}, 35), (\cdot, 5), (\phi_3^{\text{veh}}, 25), (\cdot, 5)\rangle$ assigns the time interval $[0, 35]$ s to ϕ_1^{veh}, the time interval $[40, 75]$ s to ϕ_2^{veh}, and the time interval $[80, 105]$ s to ϕ_3^{veh}, meaning that, in each of interval, the signal is green for the vehicle flow unless a tram is approaching or crossing the intersection.

For each schedule, we perform our analysis up to 5 hyper-periods (i.e., with time limit equal to $5\,H$ where $H = 220$ s) with time step $\delta = 0.1$ s, taking a total time of nearly 38 s (i.e., for the overall set of 390 schedules), and we compute the maximum expected percentage of queue occupation of any flow within the interval $[2\,H, 5\,H]$, i.e., $\bar{q}_{\text{A}}^{\max} = \max_{i\in\{1,2,3\}} \bar{Q}_{\text{A}}^{i}(t)/K \;\forall\, t \in [2\,H, 5\,H]$, where $\bar{Q}_{\text{A}}^{1}(t)$, $\bar{Q}_{\text{A}}^{2}(t)$, and $\bar{Q}_{\text{A}}^{3}(t)$ are the expected number of queued vehicles over time of ϕ_1^{veh}, ϕ_2^{veh}, and ϕ_3^{veh}, respectively. For each schedule, we also perform 25 simulation runs through the SUMO microscopic traffic simulator, requiring a total time of over 94 h (i.e., for the overall set of 390 schedules), and we also compute the maximum expected percentage $\bar{q}_{\text{S}}^{\max}$ of queue occupation of any flow.

Table 5 shows the best ten schedules computed by our analysis method, the corresponding position in the SUMO ranking, as well as the values of $\bar{q}_{\text{A}}^{\max}$ and $\bar{q}_{\text{S}}^{\max}$. Specifically, the two best schedules derived by our analysis method are the 1-st and the 4-th in the SUMO ranking, respectively, and 7 of the best 10 schedules according to our approach are in the best 10 positions in the SUMO ranking. According to this, our approach turns out to be very efficient and effective in selecting an optimal or suboptimal schedule. To further improve accuracy, SUMO simulation could be used in combination with our approach to derive the best schedule among the 5–10 top schedules provided by our analysis.

Table 5 also shows the 3 schedules in median position and the 3 worst schedules according to our analysis, still showing that the approach is suitable for comparing traffic signal schedules in terms of maximum expected percentage of queue occupation, with the worst schedule σ_{390} being the worst schedule also in the SUMO ranking. To illustrate the goodness of the optimal schedule σ_1 (which

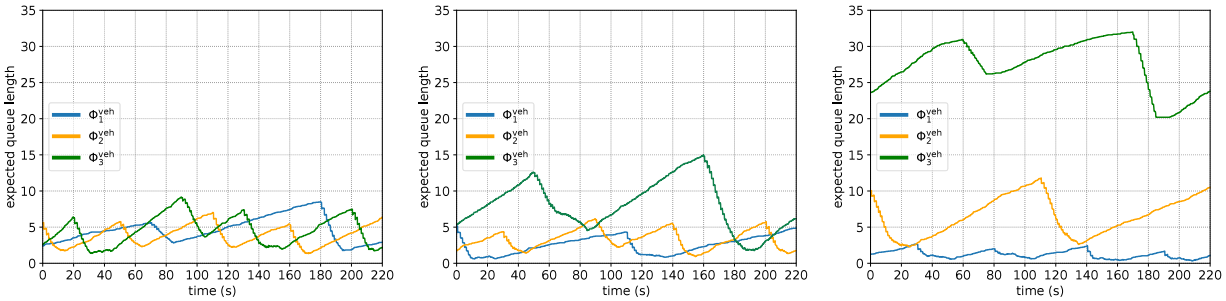

Fig. 9. Expected number of queued vehicles over time for each flow of the intersection of Table 5, computed through SUMO simulation (25 runs) for: (a) the best schedule σ_1, (b) the schedule in median position σ_{195}, and (c) the worst schedule σ_{390}.

Table 6
For a variant of the intersection of Table 5 with arrival rates $\lambda_1 = 0.1\,s^{-1}$, $\lambda_2 = 0.2\,s^{-1}$, and $\lambda_3 = 0.3\,s^{-1}$ for vehicle flows ϕ_1^{veh}, ϕ_2^{veh}, and ϕ_3^{veh}, respectively, the best 10 schedules in terms of maximum expected percentage $\bar{q}_A^{max}$ of queue occupation of any flow computed by our analysis, the maximum expected percentage $\bar{q}_S^{max}$ of queue occupation of any flow computed by SUMO simulation (25 runs), and the corresponding rank position.

Analysis rank position	$\bar{q}_A^{max}$	SUMO rank position	$\bar{q}_S^{max}$
$\sigma_1 := \langle(\phi_2^{veh}, 15), (\phi_3^{veh}, 25), (\phi_1^{veh}, 15), (\phi_2^{veh}, 15), (\phi_3^{veh}, 15)\rangle$	0.603	1	0.901
$\sigma_2 := \langle(\phi_2^{veh}, 15), (\phi_3^{veh}, 25), (\phi_2^{veh}, 15), (\phi_1^{veh}, 15), (\phi_3^{veh}, 15)\rangle$	0.603	2	0.906
$\sigma_3 := \langle(\phi_3^{veh}, 25), (\phi_2^{veh}, 15), (\phi_1^{veh}, 15), (\phi_3^{veh}, 15), (\phi_2^{veh}, 15)\rangle$	0.611	7	0.943
$\sigma_4 := \langle(\phi_3^{veh}, 25), (\phi_1^{veh}, 15), (\phi_2^{veh}, 15), (\phi_3^{veh}, 15), (\phi_2^{veh}, 15)\rangle$	0.611	4	0.932
$\sigma_5 := \langle(\phi_2^{veh}, 35), (\phi_3^{veh}, 15), (\phi_1^{veh}, 15), (\phi_3^{veh}, 25)\rangle$	0.631	14	0.961
$\sigma_6 := \langle(\phi_1^{veh}, 15), (\phi_2^{veh}, 15), (\phi_3^{veh}, 15), (\phi_2^{veh}, 15), (\phi_3^{veh}, 25)\rangle$	0.631	10	0.948
$\sigma_7 := \langle(\phi_2^{veh}, 15), (\phi_1^{veh}, 15), (\phi_3^{veh}, 15), (\phi_2^{veh}, 15), (\phi_3^{veh}, 25)\rangle$	0.631	13	0.960
$\sigma_8 := \langle(\phi_2^{veh}, 15), (\phi_3^{veh}, 15), (\phi_2^{veh}, 15), (\phi_1^{veh}, 15), (\phi_3^{veh}, 25)\rangle$	0.635	9	0.946
$\sigma_9 := \langle(\phi_2^{veh}, 15), (\phi_3^{veh}, 15), (\phi_1^{veh}, 15), (\phi_2^{veh}, 15), (\phi_3^{veh}, 25)\rangle$	0.635	19	0.965
$\sigma_{10} := \langle(\phi_3^{veh}, 25), (\phi_2^{veh}, 35), (\phi_3^{veh}, 15), (\phi_1^{veh}, 15)\rangle$	0.638	6	0.942

has maximum expected percentage of queue occupation equal to 0.297), Fig. 9 shows the expected number of queued vehicles over time of each vehicle flow computed through SUMO simulation (25 runs) over the hyper-period $[4\,H, 5\,H]$ for σ_1, for the schedule in median position σ_{195} (which has maximum expected percentage of queue occupation equal to 0.556), and for the worst schedule σ_{390} (which has maximum expected percentage of queue occupation equal to 1.0). As expected, the best schedule tends to balance the expected percentage of queue occupation of the different flows (see Fig. 9(a)). Conversely, under the worst schedule, the queue of flow ϕ_3^{veh} (green curve in Fig. 9(c)) tends to saturation, and the expected queue size of flow ϕ_2^{veh} (orange curve) is always larger than that of flow ϕ_1^{veh} (blue curve).

The experiment is repeated by increasing the arrival rates of vehicle flows ϕ_1^{veh}, ϕ_2^{veh}, and ϕ_3^{veh} to $\lambda_1 = 0.1\,s^{-1}$, $\lambda_2 = 0.2\,s^{-1}$, and $\lambda_3 = 0.3\,s^{-1}$, respectively. The experimental results reported in Table 6 show that, though the value of the maximum expected percentage of queued vehicles of any flow computed by our analysis (i.e., $\bar{q}_A^{max}$) is significantly different from that provided by SUMO (i.e., $\bar{q}_S^{max}$), the approach is still able to derive the optimal schedule. In particular, the 1-st and 2-nd schedules in our analysis ranking are the 1-st and 2-nd schedules also in the SUMO ranking, respectively, and 7 of the best 10 schedules according to our approach are in the best 10 positions in the SUMO ranking.

Table 7 reports similar results for a third variant of the initial experiment where the maximum vehicle speed is reduced to $V = 30\,km\,h^{-1}$, again showing that the approach is able to derive the optimal schedule as well as many slightly suboptimal schedules.

4.2.2. *Experiments with time-varying parameters*

We consider the intersection of Fig. 8 used in the experiments of Section 4.2.1 and we vary the tram arrival period T and the arrival rates λ_1, λ_2, and λ_3 of vehicle flows ϕ_1^{veh}, ϕ_2^{veh}, and ϕ_3^{veh}, respectively, within time intervals 1, 2, 3, and 4 corresponding to very early morning, early morning, morning, and early afternoon (to avoid saturation of queues and represent the mentioned time patterns, in this case study with three vehicle flows arrival rates are lower than in the case study of Section 4.1 with a single vehicle flow). Specifically:

- within time interval 1, $T = 440\,s$, $\lambda_1 = 0.025\,s^{-1}$, $\lambda_2 = 0.025\,s^{-1}$, and $\lambda_3 = 0.025\,s^{-1}$;
- within time interval 2, $T = 220\,s$, $\lambda_1 = 0.1\,s^{-1}$, $\lambda_2 = 0.2\,s^{-1}$, and $\lambda_3 = 0.3\,s^{-1}$;
- within time interval 3, $T = 330\,s$, $\lambda_1 = 0.05\,s^{-1}$, $\lambda_2 = 0.1\,s^{-1}$, and $\lambda_3 = 0.15\,s^{-1}$;
- within time interval 4, $T = 220\,s$, $\lambda_1 = 0.075\,s^{-1}$, $\lambda_2 = 0.15\,s^{-1}$, and $\lambda_3 = 0.2\,s^{-1}$.

We perform the analysis by assuming that the queue of each vehicle flow is empty at the initial time, and by considering that the number of queued vehicles at the beginning of each subsequent interval follows the steady-state distribution reached within the

Table 7
For a variant of the intersection of Table 5 with maximum vehicle speed $V = 30\,\mathrm{km\,h^{-1}}$, the best 10 schedules in terms of maximum expected percentage $\bar{q}_{\mathrm{A}}^{\max}$ of queue occupation of any flow computed by our analysis, the maximum expected percentage $\bar{q}_{\mathrm{S}}^{\max}$ of queue occupation of any flow computed by SUMO simulation (25 runs), and the corresponding rank position.

Analysis rank position	$\bar{q}_{\mathrm{A}}^{\max}$	SUMO rank position	$\bar{q}_{\mathrm{S}}^{\max}$
$\sigma_1 := \langle(\phi_2^{\mathrm{veh}}, 15), (\phi_3^{\mathrm{veh}}, 25), (\phi_1^{\mathrm{veh}}, 15), (\phi_2^{\mathrm{veh}}, 15), (\phi_3^{\mathrm{veh}}, 15)\rangle$	0.387	1	0.333
$\sigma_2 := \langle(\phi_2^{\mathrm{veh}}, 15), (\phi_3^{\mathrm{veh}}, 25), (\phi_2^{\mathrm{veh}}, 15), (\phi_1^{\mathrm{veh}}, 15), (\phi_3^{\mathrm{veh}}, 15)\rangle$	0.387	2	0.334
$\sigma_3 := \langle(\phi_2^{\mathrm{veh}}, 15), (\phi_3^{\mathrm{veh}}, 15), (\phi_2^{\mathrm{veh}}, 15), (\phi_1^{\mathrm{veh}}, 15), (\phi_3^{\mathrm{veh}}, 25)\rangle$	0.410	3	0.353
$\sigma_4 := \langle(\phi_2^{\mathrm{veh}}, 15), (\phi_3^{\mathrm{veh}}, 15), (\phi_1^{\mathrm{veh}}, 15), (\phi_2^{\mathrm{veh}}, 15), (\phi_3^{\mathrm{veh}}, 25)\rangle$	0.410	5	0.360
$\sigma_5 := \langle(\phi_1^{\mathrm{veh}}, 15), (\phi_3^{\mathrm{veh}}, 15), (\phi_2^{\mathrm{veh}}, 35), (\phi_3^{\mathrm{veh}}, 25)\rangle$	0.414	24	0.396
$\sigma_6 := \langle(\phi_3^{\mathrm{veh}}, 25), (\phi_2^{\mathrm{veh}}, 35), (\phi_3^{\mathrm{veh}}, 15), (\phi_1^{\mathrm{veh}}, 15)\rangle$	0.416	20	0.393
$\sigma_7 := \langle(\phi_3^{\mathrm{veh}}, 25), (\phi_2^{\mathrm{veh}}, 15), (\phi_1^{\mathrm{veh}}, 15), (\phi_3^{\mathrm{veh}}, 15), (\phi_2^{\mathrm{veh}}, 15)\rangle$	0.416	10	0.373
$\sigma_8 := \langle(\phi_3^{\mathrm{veh}}, 25), (\phi_1^{\mathrm{veh}}, 15), (\phi_2^{\mathrm{veh}}, 15), (\phi_3^{\mathrm{veh}}, 15), (\phi_2^{\mathrm{veh}}, 15)\rangle$	0.416	12	0.376
$\sigma_9 := \langle(\phi_2^{\mathrm{veh}}, 35), (\phi_3^{\mathrm{veh}}, 15), (\phi_1^{\mathrm{veh}}, 15), (\phi_3^{\mathrm{veh}}, 25)\rangle$	0.417	9	0.369
$\sigma_{10} := \langle(\phi_1^{\mathrm{veh}}, 15), (\phi_2^{\mathrm{veh}}, 15), (\phi_3^{\mathrm{veh}}, 15), (\phi_2^{\mathrm{veh}}, 15), (\phi_3^{\mathrm{veh}}, 25)\rangle$	0.417	4	0.359

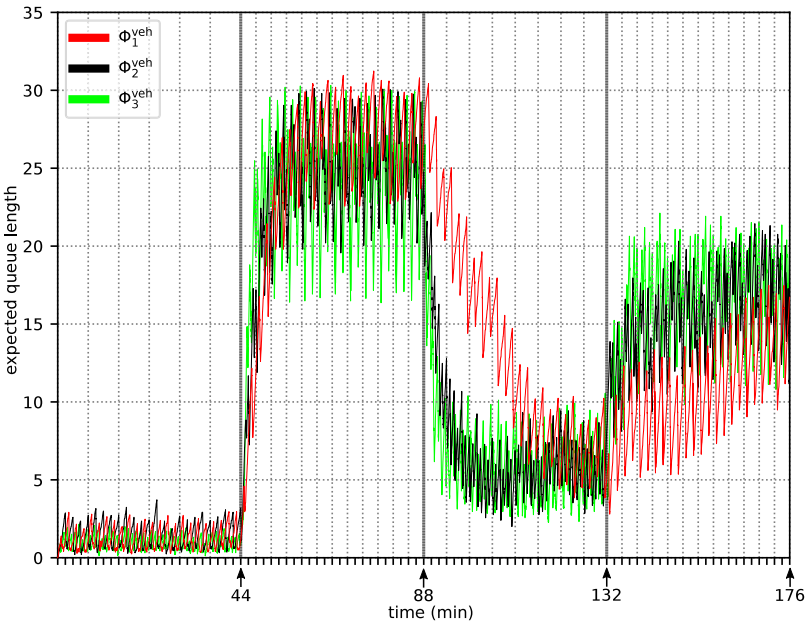

Fig. 10. Expected queue length over time computed by SUMO simulation (25 runs) for each flow of the intersection of Fig. 8, considering time-varying vehicle arrival rates and tram departure period over 4 intervals of 44 min duration each, assuming the optimal schedules (at minimizing the maximum expected percentage of queued vehicles of each flow) derived by our analysis.

previous interval at multiples of the hyper-period. For each time interval, we repeat the analysis for the duration of one hyper-period for each of the 390 signal schedules defined in Section 4.2.1 and we derive the optimal schedule at minimizing the maximum expected percentage of queued vehicles of each flow, which takes a total time of nearly 3.5 min. Note that, being $P = 110\,\mathrm{s}$ the period of the intersection traffic light, the hyper-period duration is $H_1 = 440\,\mathrm{s}$, $H_2 = 220\,\mathrm{s}$, $H_3 = 330\,\mathrm{s}$, and $H_4 = 220\,\mathrm{s}$ for time intervals 1, 2, 3, and 4, respectively.

Then, we perform 25 SUMO simulation runs (as in the experiments of Section 4.2.1) to compute the expected queue size over time for each flow, by considering in each time interval the optimal traffic signal schedule derived by our analysis method, and by assuming that each time interval lasts 44 min, corresponding to the duration of 6 hyper-periods, 12 hyper-periods, 8 hyper-periods, and 12 hyper-periods for time intervals 1, 2, 3, and 4, respectively. SUMO simulation takes a total time of nearly 2 h. Fig. 10 plots the results, showing that the expected number of queued vehicles of each flow is larger for the time intervals 2 and 4 during which the tram arrival period is lower and the vehicle arrival rates are larger with respect to the time intervals 1 and 3. Also note that, in each time interval, the selected traffic signal schedule tends to balance the expected percentage of queue occupation of the three flows at the steady-state. In particular, the curves show that the steady state is always reached within few hyper-periods, at most nearly a dozen hyper-periods in cases with greater variations in parameter values between subsequent time intervals: in time interval 1, starting from empty queue and having low arrival rate and large tram period, the steady state is reached almost immediately; in time interval 2, it takes 4–5 hyper-periods, due to the larger arrival rates and lower tram period; in time intervals 3 and 4, a few more hyper-periods are needed for all flows to reach the steady state, due to the different load condition in the previous time interval, i.e., in time intervals 2 and 3, respectively. Note that performing SUMO simulation runs spanning across multiple time intervals avoids the problem of computing, for each time interval, the steady-state distribution of the expected queue size of each

flow at multiples of the hyper-period, which would be almost unfeasible to perform through SUMO simulation, and actually prevents exploiting SUMO to derive optimal signal schedules especially when system parameters vary over time.

5. Conclusions

This paper presents an efficient compositional approach for offline derivation of optimal signal schedules for multimodal intersections among road vehicle flows and tram lines with right of way, minimizing the maximum expected percentage of queued vehicles of each flow. To derive the expected queue size over time of each vehicle flow, transient analyses of microscopic models of tram traffic, capturing deterministic and GEN temporal parameters of the arrival and travel processes of trams, are composed with transient analyses of macroscopic models of road vehicle flows, leveraging finite-capacity vacation queues with GEN vacation time. We prove that the distribution of the expected number of queued vehicles of each flow at multiples of the hyper-period (i.e., the least common multiple of the periods of tram departures and vehicle signals) reaches a steady state, which is experimentally observed to be reached within few hyper-periods. Therefore, the expected queue size over time of each flow can be completely characterized by performing transient analysis starting from the computed steady-state distribution for the duration of one hyper-period, enabling efficient evaluation of performance with time-varying parameters over intervals of arbitrary duration.

The results achieved in the evaluation of the expected queue size over time are validated with respect to those obtained through SUMO, showing that the approach is very efficient and sufficiently accurate for the context of use, and that the analysis achieves better accuracy when vehicle flows are modeled by M/M/K/K than M/M/1/K vacation queues with GEN vacation time. In particular, in less than 2.7 s, the analysis achieves NRMSD lower than 0.37 in the worst case, lower than 0.2 in more than 80% of the cases, and lower than 0.1 in nearly 50% of the cases, compared to SUMO simulation which takes tens of seconds to achieve comparable NRMSD. Results also show that the approach is able to capture peaks and troughs of the expected number of queued vehicles over time, as well as relative variations as values of parameters change, appearing suitable to derive optimal schedules for vehicle signals, and promising to address more complex scenarios where inter-arrival times of road vehicles are characterized by GEN distributions.

Experimental results show that the approach derives optimal signal schedules by analyzing hundreds of schedules in few minutes, which requires tens of hours in SUMO. Moreover, the approach can be effectively used to derive optimal schedules also when the system parameters vary over time, exploiting transient analysis starting from the steady-state distribution of the expected queue size over time, which would be almost unfeasible to compute using a microscopic traffic simulator like SUMO. According to this, simulation of microscopic models of the entire multimodal intersection appears much more suitable to derive accurate quantitative measures of interest given specific values of the system parameters rather than to explore the design space of the system parameters, especially when the values of system parameters vary over time.

The availability of finer statistics of arrival times and travel times, both for trams and for road vehicles, would improve fitting of durations with more accurate probability distributions, enabling full exploitation of the proposed approach. Actually, these data are becoming easier to collect by urban transport operators thanks to the growing deployment of smart technologies [60,61,74]. Then, various approaches can be used to derive expolynomial duration CDFs, fitting either moments [75] or shape [76,77] of observed data.

Achieved results enable future works including application of the approach to evaluate the impact of different traffic signal policies on performance of road transport and tram transport, such as model predictive control mechanisms to adapt the operational parameters at runtime according to measured traffic variables. The approach also lays a ground for joint optimization of traffic signal schedules for multiple, possibly multimodal, connected intersections within a urban transportation network. In particular, the approach could be extended also by considering multi-lane vehicle flows and by integrating statistical information about vehicle movements, exploiting approaches that, with different objectives, investigate two-dimensional paths of vehicles while approaching or crossing an intersection, e.g., microscopic behavioral models are exploited to describe unprotected left-turn movements in [78] and interactions between drivers in [79], spatio-temporal characteristics like lateral movements and vehicle following time are considered in [80] to analyze rear-end conflicts, and vehicle static and dynamic characteristics are used in [81] to estimate saturation flow. Future work would also include validation with respect to microscopic traffic simulators able to represent variability in vehicle movements.

Data availability

The OMNIBUS Java library is available open source under the AGPLv3 licence at https://doi.org/10.5281/zenodo.10693840, supporting replication of the experimental results. A repository supporting replication of the comparison of the experimental results with those obtained by SUMO is available under the EPLv2 licence at https://doi.org/10.5281/zenodo.10695718.

Acknowledgements

This work was partially supported by the European Union under the Italian National Recovery and Resilience Plan (NRRP) of NextGenerationEU, partnership on “Telecommunications of the Future” (PE00000001 - program “RESTART”).

References

[1] R. Balcombe, R. Mackett, N. Paulley, J. Preston, J. Shires, H. Titheridge, M. Wardman, P. White, The Demand for Public Transport: A Practical Guide, Transportation Research Laboratory, 2004.
[2] ERTRAC, Integrated Urban Mobility Roadmap, Technical Report, European Road Transport Research Advisory Council, 2017.
[3] ACEA, The 2030 Urban Mobility Challenge, Technical Report, 2016.
[4] R. Faria, L. Brito, K. Baras, J. Silva, Smart mobility: A survey, in: Int. Conf. on IoT for the Global Community, IEEE, 2017, pp. 1–8.
[5] C. Cheng, Y. Du, L. Sun, Y. Ji, Review on theoretical delay estimation model for signalized intersections, Transp. Rev. 36 (4) (2016) 479–499.
[6] M. Eom, B.-I. Kim, The traffic signal control problem for intersections: A review, Eur. Transp. Res. Rev. 12 (2020) 1–20.
[7] K.M. Ng, M.B.I. Reaz, M.A.M. Ali, A review on the applications of Petri nets in modeling, analysis, and control of urban traffic, IEEE Trans. on Int. Transp. Sys. 14 (2) (2013) 858–870, http://dx.doi.org/10.1109/TITS.2013.2246153.
[8] S. Maerivoet, B. De Moor, Cellular automata models of road traffic, Phys. Rep. 419 (1) (2005) 1–64.
[9] Y. Li, D. Sun, Microscopic car-following model for the traffic flow: The state of the art, J. Contr. Theory Appl. 10 (2) (2012) 133–143.
[10] F.V. Webster, Traffic signal settings. Road Research Technical Paper 39, Technical Report, 1958.
[11] M.J. Lighthill, G.B. Whitham, On kinematic waves II. A theory of traffic flow on long crowded roads, Proc. R. Soc. Lond. Ser. A. 229 (1178) (1955) 317–345.
[12] G. Stephanopoulos, P.G. Michalopoulos, G. Stephanopoulos, Modelling and analysis of traffic queue dynamics at signalized intersections, Transp. Res. A 13 (5) (1979) 295–307.
[13] F. Dion, B. Hellinga, A rule-based real-time traffic responsive signal control system with transit priority: Application to an isolated intersection, Transport. Res. B 36 (4) (2002) 325–343.
[14] S. Yagar, B. Han, J. Greenough, Real-time signal control. for mixed traffic and transit based on priority rules, in: Traffic Management. Proc. of the Eng. Foundation Conference, 1992.
[15] A. Di Febbraro, N. Sacco, On modelling urban transportation networks via hybrid Petri nets, Control Eng. Practices 12 (10) (2004) 1225–1239, http://dx.doi.org/10.1016/j.conengprac.2004.04.008, URL: http://www.sciencedirect.com/science/article/pii/S096706610400084X.
[16] A. Di Febbraro, D. Giglio, N. Sacco, Urban traffic control structure based on hybrid Petri nets, IEEE Tr. Int. Tran. Sys. 5 (4) (2004) 224–237, http://dx.doi.org/10.1109/TITS.2004.838180.
[17] M. Dotoli, M.P. Fanti, G. Iacobellis, An urban traffic network model by first order hybrid Petri nets, in: 2008 IEEE Int. Conf. on Systems, Man and Cybernetics, IEEE, 2008, pp. 1929–1934.
[18] C. Tolba, D. Lefebvre, P. Thomas, A. El Moudni, Continuous and timed Petri nets for the macroscopic and microscopic traffic flow modelling, Simul. Model. Practice Theory 13 (5) (2005) 407–436.
[19] Y. Zhang, R. Su, An optimization model and traffic light control scheme for heterogeneous traffic systems, Transp. Res. C 124 (2021) 102911.
[20] A. Sharma, D.M. Bullock, J.A. Bonneson, Input–output and hybrid techniques for real-time prediction of delay and maximum queue length at signalized intersections, Transp. Res. Rec. 2035 (1) (2007) 69–80.
[21] P.G. Michalopoulos, G. Stephanopoulos, G. Stephanopoulos, An application of shock wave theory to traffic signal control, Transp. Res. B 15 (1) (1981) 35–51.
[22] A. Di Febbraro, D. Giglio, On representing signalized urban areas by means of deterministic-timed Petri nets, in: Int. Conf. on Intelligent Transportation Systems, 2004, pp. 372–377.
[23] A. Di Febbraro, D. Giglio, N. Sacco, A deterministic and stochastic Petri net model for traffic-responsive signaling control in urban areas, IEEE Trans. on Int. Transp. Sys. 17 (2) (2016) 510–524, http://dx.doi.org/10.1109/TITS.2015.2478602.
[24] L. Carnevali, A. Fantechi, G. Gori, E. Vicario, Stochastic modeling and analysis of road–tramway intersections, Innov. Syst. Softw. Eng. 16 (2) (2020) 215–230.
[25] L. Carnevali, A. Fantechi, G. Gori, E. Vicario, Analysis of a road/tramway intersection by the ORIS tool, in: Int. Conf. on Verif. and Eval. of Computer and Comm. Systems, Springer, 2018, pp. 185–199.
[26] C. Portilla, F. Valencia, J. Espinosa, A. Nunez, B. De Schutter, Model-based predictive control for bicycling in urban intersections, Transp. Res. C 70 (2016) 27–41.
[27] Q. He, K.L. Head, J. Ding, Multi-modal traffic signal control with priority, signal actuation and coordination, Transp. Res. C 46 (2014) 65–82.
[28] M. Fellendorf, VISSIM: A microscopic simulation tool to evaluate actuated signal control including bus priority, in: 64th Institute of Transportation Engineers Annual Meeting, vol. 32, Springer, 1994, pp. 1–9.
[29] J. Stevanovic, A. Stevanovic, P.T. Martin, T. Bauer, Stochastic optimization of traffic control and transit priority settings in VISSIM, Transp. Res. C 16 (3) (2008) 332–349.
[30] J. Shi, Y. Sun, P. Schonfeld, J. Qi, Joint optimization of tram timetables and signal timing adjustments at intersections, Transp. Res. C 83 (2017) 104–119.
[31] Y. Ji, Y. Tang, Y. Du, X. Zhang, Coordinated optimization of tram trajectories with arterial signal timing resynchronization, Transp. Res. C 99 (2019) 53–66.
[32] T. Zhang, B. Mao, Q. Xu, J. Feng, Timetable optimization for a two-way tram line with an active signal priority strategy, IEEE Access 7 (2019) 176896–176911.
[33] O.K. Tonguz, W. Viriyasitavat, F. Bai, Modeling urban traffic: A cellular automata approach, IEEE Comm. Maga. 47 (5) (2009) 142–150.
[34] L. Zhang, T. Garoni, A comparison of tram priority at signalized intersections, 2013, arXiv preprint arXiv:1311.3590.
[35] Q. Guo, L. Li, X.J. Ban, Urban traffic signal control with connected and automated vehicles: A survey, Transp. Res. C 101 (2019) 313–334.
[36] Z. Li, L. Elefteriadou, S. Ranka, Signal control optimization for automated vehicles at isolated signalized intersections, Transp. Res. C 49 (2014) 1–18.
[37] M. Pourmehrab, L. Elefteriadou, S. Ranka, M. Martin-Gasulla, Optimizing signalized intersections performance under conventional and automated vehicles traffic, IEEE Trans. Intell. Transp. Syst. 21 (7) (2019) 2864–2873.
[38] R. Reddy, L. Almeida, M.G. Gaitán, P.M. Santos, E. Tovar, Synchronous management of mixed traffic at signalized intersections towards sustainable road transportation, IEEE Access (2023).
[39] Y. Ji, Y. Tang, Y. Shen, Y. Du, W. Wang, An integrated approach for tram prioritization in signalized corridors, IEEE Trans. Intell. Transp. Syst. 21 (6) (2019) 2386–2395.
[40] H. Wei, G. Zheng, V. Gayah, Z. Li, A survey on traffic signal control methods, 2019, arXiv preprint arXiv:1904.08117.
[41] P. Balaji, D. Srinivasan, Multi-agent system in urban traffic signal control, IEEE Comput. Intell. Mag. 5 (4) (2010) 43–51.
[42] K. Prabuchandran, H.K. AN, S. Bhatnagar, Multi-agent reinforcement learning for traffic signal control, in: Int. IEEE Conf. on Intelligent Transportation Systems, IEEE, 2014, pp. 2529–2534.
[43] T. Chu, J. Wang, L. Codecà, Z. Li, Multi-agent deep reinforcement learning for large-scale traffic signal control, IEEE Tran. Intell. Transp. Syst. 21 (3) (2019) 1086–1095.
[44] P.A. Lopez, M. Behrisch, L. Bieker-Walz, J. Erdmann, Y.-P. Flötteröd, R. Hilbrich, L. Lücken, J. Rummel, P. Wagner, E. Wießner, Microscopic traffic simulation using SUMO, in: Int. Conf. on Intelligent Transportation Systems, IEEE, 2018, pp. 2575–2582.

[45] E. Vicario, L. Sassoli, L. Carnevali, Using stochastic state classes in quantitative evaluation of dense-time reactive systems, IEEE Trans. Softw. Eng. 35 (5) (2009) 703–719.
[46] A. Horváth, M. Paolieri, L. Ridi, E. Vicario, Transient analysis of non-Markovian models using stochastic state classes, Perform. Eval. 69 (7–8) (2012) 315–335, http://dx.doi.org/10.1016/j.peva.2011.11.002.
[47] N. Tian, Z.G. Zhang, Vacation Queueing Models: Theory and Applications, vol. 93, Springer Science & Business Media, 2006.
[48] L. Kleinrock, R. Gail, Queueing Systems: Theory, vol. 1, Wiley, New York, 1975.
[49] G. Bolch, S. Greiner, H. De Meer, K.S. Trivedi, Queueing Networks and Markov Chains: Modeling and Performance Evaluation with Computer Science Applications, John Wiley & Sons, 2006.
[50] A.R. Da Silva, Model-driven engineering: A survey supported by the unified conceptual model, Comp. Lang., Sys. Struct. 43 (2015) 139–155.
[51] Y. Lin, X. Yang, N. Zou, M. Franz, Transit signal priority control at signalized intersections: A comprehensive review, Transp. Lett. 7 (3) (2015) 168–180.
[52] C. Lindemann, A. Thümmler, Transient analysis of deterministic and stochastic Petri nets with concurrent deterministic transitions, Perform. Eval. 36–37 (1–4) (1999) 35–54, http://dx.doi.org/10.1016/S0166-5316(99)00020-6.
[53] A. Horvath, A. Puliafito, M. Scarpa, M. Telek, Analysis and evaluation of non-Markovian stochastic Petri nets, in: Proc. Int. Conf. Computer Performance Evaluation, 2000, pp. 171–187, http://dx.doi.org/10.1007/3-540-46429-8_13.
[54] F. Longo, M. Scarpa, Applying symbolic techniques to the representation of non-Markovian models with continuous PH distributions, in: Proc. European Perf. Eng. Workshop, Springer, 2009, pp. 44–58, http://dx.doi.org/10.1007/978-3-642-02924-0_4.
[55] K.S. Trivedi, R. Sahner, SHARPE at the age of twenty two, SIGMETRICS Perform. Eval. Rev. 36 (4) (2009) 52–57, http://dx.doi.org/10.1145/1530873.1530884.
[56] M. Paolieri, M. Biagi, L. Carnevali, E. Vicario, The ORIS tool: Quantitative evaluation of non-Markovian systems, IEEE Trans. Softw. Eng. 47 (6) (2021) 1211–1225.
[57] SIRIO Library, 2023. https://github.com/oris-tool/sirio.
[58] GEST, 2023. https://gestramvia.it/company/?lang=en.
[59] S. Bernardi, J. Campos, J. Merseguer, Timing-failure risk assessment of UML design using time Petri net bound techniques, IEEE Trans. Ind. Inf. 7 (1) (2011) 90–104, http://dx.doi.org/10.1109/TII.2010.2098415.
[60] M. Luckner, J. Karwowski, Estimation of delays for individual trams to monitor issues in public transport infrastructure, in: Int. Conf. on Computational Collective Intelligence, Springer, 2017, pp. 518–527.
[61] A. Zychowski, K. Junosza-Szaniawski, A. Kosicki, Travel time prediction for trams in Warsaw, in: International Conference on Computer Recognition Systems, Springer, 2018, pp. 53–62.
[62] J.-C. Ke, C.-H. Wu, Z.G. Zhang, Recent developments in vacation queueing models: A short survey, Int. J. Oper. Res. 7 (4) (2010) 3–8.
[63] B.T. Doshi, Queueing systems with vacations—A survey, Queueing Syst. 1 (1986) 29–66.
[64] O.C. Ibe, K.S. Trivedi, Stochastic Petri net analysis of finite-population vacation queueing systems, Queueing Syst. 8 (1) (1991) 111–127.
[65] O.C. Ibe, K.S. Trivedi, Stochastic Petri net models of polling systems, IEEE J. Sel. Areas Comm. 8 (9) (1990) 1649–1657.
[66] N. Tian, Z.G. Zhang, Stationary distributions of GI/M/c queue with PH type vacations, Queueing Syst. 44 (2003) 183–202.
[67] N. Prabhu, Y. Zhu, Markov-modulated queueing systems, Queueing Syst. 5 (1989) 215–245.
[68] M. Woodside, Queue response times with server speed controlled by measured utilizations, in: Proc. QEST, Springer, 2021, pp. 295–309.
[69] M.F. Neuts, A versatile Markovian point process, J. Appl. Probab. 16 (4) (1979) 764–779.
[70] S.R. Chakravarthy, Analysis of a multi-server queue with Markovian arrivals and synchronous phase type vacations, Asia-Pac. J. Oper. Res. 26 (01) (2009) 85–113.
[71] S.R. Chakravarthy, A multi-server synchronous vacation model with thresholds and a probabilistic decision rule, European J. Oper. Res. 182 (1) (2007) 305–320.
[72] W.J. Stewart, Introduction to the Numerical Solution of Markov Chains, Princeton University Press, 1994.
[73] S. Krauß, Microscopic modeling of traffic flow: Investigation of collision free vehicle dynamics, 1998.
[74] Y. Byon, A. Shalaby, B. Abdulhai, Travel time collection and traffic monitoring via GPS technologies, in: 2006 IEEE Intelligent Transportation Systems Conference, IEEE, 2006, pp. 677–682.
[75] W. Whitt, Approximating a point process by a renewal process, I: Two basic methods, Oper. Res. 30 (1) (1982) 125–147.
[76] P. Reinecke, T. Krauß, K. Wolter, Phase-type fitting using HyperStar, in: European Workshop on Computer Performance Engineering, Springer, 2013, pp. 164–175.
[77] A. Horváth, M. Telek, Phfit: A general phase-type fitting tool, in: Int. Conf. on Modelling Techniques and Tools for Computer Performance Evaluation, Springer, 2002, pp. 82–91.
[78] J. Zhao, V.L. Knoop, J. Sun, Z. Ma, M. Wang, Unprotected left-turn behavior model capturing path variations at intersections, IEEE Trans. Intell. Transp. Syst. (2023).
[79] J. Zhao, V.L. Knoop, M. Wang, Microscopic traffic modeling inside intersections: Interactions between drivers, Transp. Sci. 57 (1) (2023) 135–155.
[80] R. Chauhan, A. Dhamaniya, S. Arkatkar, Spatiotemporal variation of rear-end conflicts at signalized intersections under disordered traffic conditions, J. Transport. Eng. A: Systems 147 (11) (2021) 05021007.
[81] R.K. Padinjarapat, T.V. Mathew, Estimation of saturation flow for non-lane based mixed traffic streams, Transportmetrica B 9 (1) (2021) 42–61.